AD-A051 132 CALIFORNIA UNIV SAN DIEGO LA JOLLA DEPT OF APPLIED M--ETC F/G 11/4
MECHANICS OF COMPOSITE MATERIALS.(U)
1977 G A HEGEMIER F49620-76-C-0024

UNCLASSIFIED AFOSR-TR-78-0206 NL

1 OF 1
ADA
051132

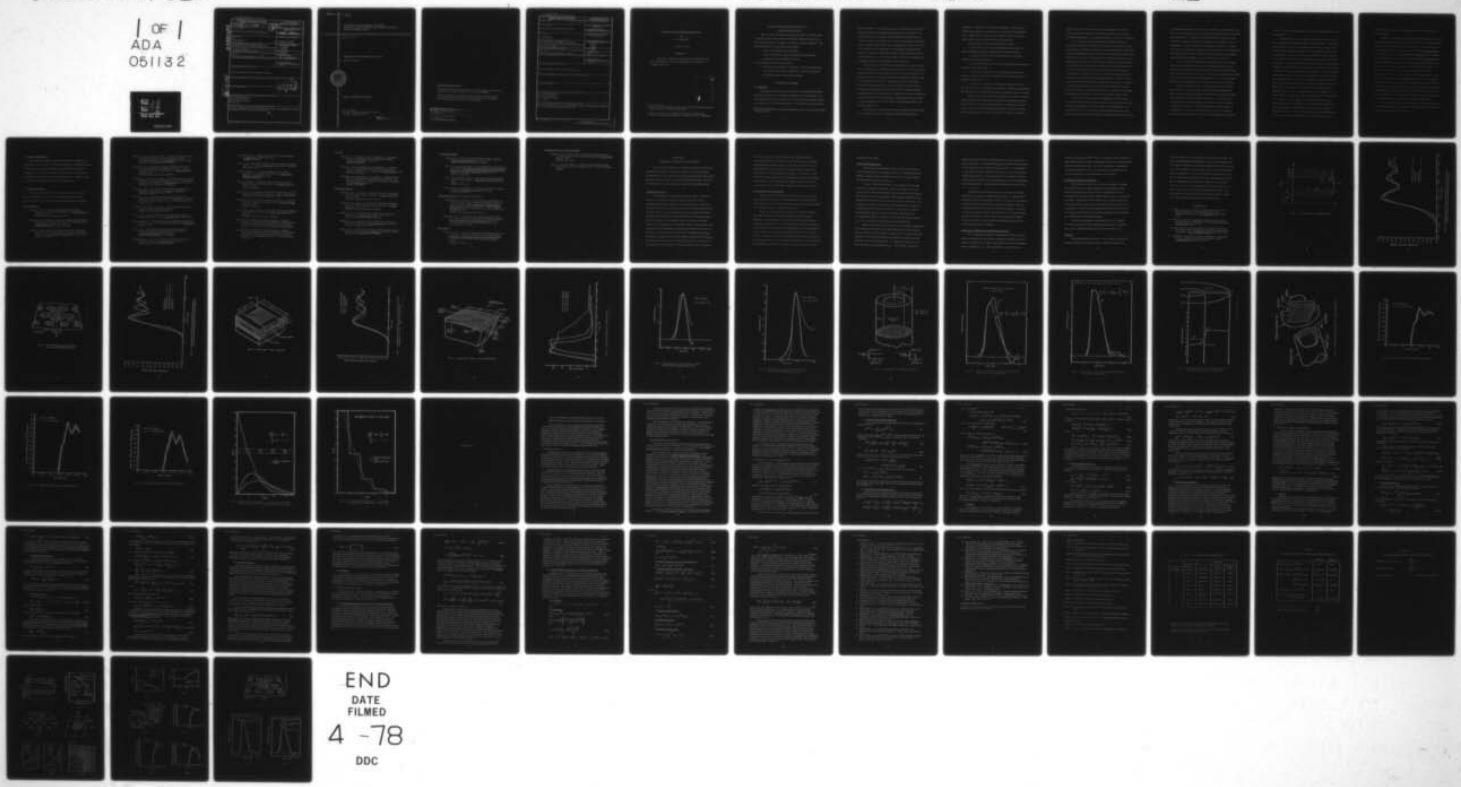

END
DATE
FILMED
4 -78
DDC

UNCLASSIFIED

SECURITY CLASSIFICATION OF THIS PAGE (When Data Entered)

AD A051132

DDC FILE COPY

REPORT DOCUMENTATION PAGE	READ INSTRUCTIONS BEFORE COMPLETING FORM
1. REPORT NUMBER: AFOSR-TR-78-0206	2. GOVT ACCESSION NO.	3. RECIPIENT'S CATALOG NUMBER
4. TITLE (and Subtitle): MECHANICS OF COMPOSITE MATERIALS.	5. TYPE OF REPORT & PERIOD COVERED: Annual technical INTERIM rept. July 1976 - June 1977
	6. PERFORMING ORG. REPORT NUMBER
7. AUTHOR(s): G A HEGEMIER	8. CONTRACT OR GRANT NUMBER(s): F49620-76-C-0024
9. PERFORMING ORGANIZATION NAME AND ADDRESS: UNIVERSITY OF CALIFORNIA, SAN DIEGO, APPLIED MECHANICS & ENGINEERING SCIENCE DEP, LA JOLLA, CA 92093	10. PROGRAM ELEMENT, PROJECT, TASK AREA & WORK UNIT NUMBERS: 2307B1, 61102F
11. CONTROLLING OFFICE NAME AND ADDRESS: AIR FORCE OFFICE OF SCIENTIFIC RESEARCH/NA, BLDG 410, BOLLING AIR FORCE BASE, D C 20332	12. REPORT DATE: 1977
	13. NUMBER OF PAGES: 68 (71 p.)
14. MONITORING AGENCY NAME & ADDRESS (if different from Controlling Office)	15. SECURITY CLASS. (of this report): UNCLASSIFIED
	15a. DECLASSIFICATION/DOWNGRADING SCHEDULE

16. DISTRIBUTION STATEMENT (of this Report)

Approved for public release; distribution unlimited.

17. DISTRIBUTION STATEMENT (of the abstract entered in Block 20, if different from Report)

DDC RECEIVED MAR 10 1978 F

18. SUPPLEMENTARY NOTES

19. KEY WORDS (Continue on reverse side if necessary and identify by block number)

COMPOSITE MATERIALS
WAVE PROPAGATION
MECHANICS OF FAILURE
DIFFUSION

20. ABSTRACT (Continue on reverse side if necessary and identify by block number)

This report summarizes the results of a theoretical study of wave propagation, diffusion, and damage accumulation in composite materials.

DD FORM 1473 EDITION OF 1 NOV 65 IS OBSOLETE

407 513

UNIVERSITY OF CALIFORNIA, SAN DIEGO
Department of Applied Mechanics and Engineering Sciences
La Jolla, California 92093

F49620-76-C-0024

MECHANICS OF COMPOSITE MATERIALS

by G. A. Hegemier

ANNUAL TECHNICAL REPORT

Prepared for
Air Force Office of Scientific Research
Arlington, Virginia 22209

UNCLASSIFIED

SECURITY CLASSIFICATION OF THIS PAGE *(When Data Entered)*

REPORT DOCUMENTATION PAGE		READ INSTRUCTIONS BEFORE COMPLETING FORM
1. REPORT NUMBER	2. GOVT ACCESSION NO.	3. RECIPIENT'S CATALOG NUMBER
4. TITLE *(and Subtitle)* MECHANICS OF COMPOSITE MATERIALS		5. TYPE OF REPORT & PERIOD COVERED INTERIM July 1976 - June 1977 6. PERFORMING ORG. REPORT NUMBER
7. AUTHOR(s) G A HEGEMIER		8. CONTRACT OR GRANT NUMBER(s) F49620-76-C-0024
9. PERFORMING ORGANIZATION NAME AND ADDRESS UNIVERSITY OF CALIFORNIA, SAN DIEGO APPLIED MECHANICS & ENGINEERING SCIENCE DEP LA JOLLA, CA 92093		10. PROGRAM ELEMENT, PROJECT, TASK AREA & WORK UNIT NUMBERS 2307B1 61102F
11. CONTROLLING OFFICE NAME AND ADDRESS AIR FORCE OFFICE OF SCIENTIFIC RESEARCH/NA BLDG 410 BOLLING AIR FORCE BASE, D C 20332		12. REPORT DATE 1977 13. NUMBER OF PAGES 68
14. MONITORING AGENCY NAME & ADDRESS*(if different from Controlling Office)*		15. SECURITY CLASS. *(of this report)* UNCLASSIFIED 15a. DECLASSIFICATION/DOWNGRADING SCHEDULE

16. DISTRIBUTION STATEMENT *(of this Report)*

Approved for public release; distribution unlimited.

17. DISTRIBUTION STATEMENT *(of the abstract entered in Block 20, if different from Report)*

18. SUPPLEMENTARY NOTES

19. KEY WORDS *(Continue on reverse side if necessary and identify by block number)*

COMPOSITE MATERIALS
WAVE PROPAGATION
MECHANICS OF FAILURE
DIFFUSION

20. ABSTRACT *(Continue on reverse side if necessary and identify by block number)*

This report summarizes the results of a theoretical study of wave propagation, diffusion, and damage accumulation in composite materials.

DD FORM 1 JAN 73 1473 EDITION OF 1 NOV 65 IS OBSOLETE

UNCLASSIFIED

SECURITY CLASSIFICATION OF THIS PAGE *(When Data Entered)*

MECHANICS OF COMPOSITE MATERIALS[†]

by

G. A. Hegemier[1]

F49620-76-C-0024

ABSTRACT

This report summarizes the results of a theoretical study of wave propagation, diffusion, and damage accumulation in composite materials.

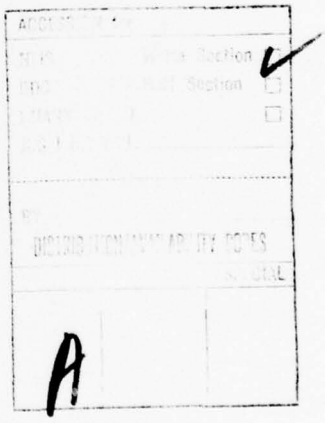

[†] Sponsored by the United States Air Force Office of Scientific Research, at the University of California, San Diego.

[1] Professor, Department of Applied Mechanics and Engineering Sciences, University of California, San Diego, La Jolla, California.

MECHANICS OF COMPOSITE MATERIALS

1. RESEARCH OBJECTIVES

Research under the subject Contract represents a continuing effort[3] to construct viable nonlinear micro-mechanical continuum models to predict the thermomechanical response of advanced composite materials. The thermomechanical processes under study include:

- Linear and nonlinear wave propagation
- Linear and nonlinear diffusion (thermal and hygrothermal)
- Mechanisms and accumulation of damage.

The thermomechanical measures include:

- Global stress, deformation, temperature, internal energy fields
- Local stress, deformation, temperature, internal energy fields
- Residual properties of damaged composites.

2. RESEARCH PROGRESS

2.1 Discussion

Excellent progress has been made to date in modeling both laminated and fibrous composites as homogeneous continua with microstructure. The resulting theory is generally referred to as a "Theory of Interacting Continua" or a "Mixture Theory with Microstructure". In contrast to classical theories

[3] Previous work was conducted under AF-AFOSR Grant 70-1975 and AF-AFOSR Contract 75-2870.

with similar titles, the governing equations are completely specified by a knowledge of the initial microstructural geometry of the composite, the component constitutive relations, and the component interface physics. In further contrast to classical theories, the current model provides information on stress, displacement, strain, temperature, and internal energy fields within the microcomponents as well as global measures of these quantities. The present theory also accounts for debonding at the microcomponent interfaces - a basic damage mode. Models incorporating crack distributions throughout the constituents are under study.

The most general mathematical model considered to date is a nonlinear, anisotropic, thermomechanical mixture theory with microstructure. Particular, simplified forms of this model have been developed to cover special cases of composite geometry, material constitutive relations, and physical processes or problems. In all cases, however, theoretical construction is based upon one of two basic methods which are in turn based upon an asymptotic scheme in which dominant signal wavelengths associated with the physical process are assumed to be large in comparison with typical composite microdimensions. An explanation of the foregoing construction methods, as well as a number of interesting examples, can be found in Appendix II.

The composites studied using the above asymptotic technique range from elementary laminated to complex three-dimensional advanced

composites. In addition to certain model composites, materials have included quartz phenolic, carbon phenolic, carbon carbon, and graphite epoxy. Representative problem areas include nose tips, heat shields, engine blades, nozzles, and hygrothermal environments.

Cases completed and in publication thus far include:

. A general theory for wave propagation in linear elastic and linear-viscoelastic laminated composites with isotropic laminae;

. A general theory for linear thermal diffusion in laminated composites with isotropic laminae;

. A "first order" theory for linear wave propagation in anisotropic laminates with oblique layup;

. "First order" theories for wave propagation, diffusion, and debonding in unidirectional fibrous composites with cylindrical fibers of arbitrary cross section;

. "First order" nonlinear, anisotropic and isotropic, thermodynamic theories for wave propagation, diffusion, and damage accumulation due to debonding in both laminated and fibrous composites of specific types.

In the general linear cases above, a hierarchy of models is systematically defined by the order of the truncation of the asymptotic sequence involved in the theoretical construction process. Retention of all terms in this sequence leads to a formally exact theory. Retention of only the zeroth-order plus first order terms results in a so-called "first order"

theory which can be cast in the form of a mixture theory. The latter usually constitutes an adequate micromechanical model of a composite for engineering purposes. All nonlinear models are "first order" theories.

The first order models for laminates and fibrous composites incorporate the effects of arbitrary fiber geometry, anisotropy, and interface debonding. In addition to diffusion, a thermodynamic theory of elastic-plastic wave propagation under finite deformation has been developed. The constitutives laws of the microcomponents currently in publication relate the mean stress (trace of the stress tensor) to density and internal energy by a Mie-Grüneisen caloric equation of state and the stress deviator tensor to the rate-of-deformation tensor by an elastic-perfectly plastic relation of the von Mises type; extension to general anisotropic plasticity utilizing a plastic potential and an associated flow ride is under development. Constituent debonding and component-interface physics is governed by a Coulomb frictional-type relation; the latter constitutes the present measure of "damage"; extension of this measure to include microcracking throughout the components is, as was noted previously, under study.

In the case of linear elastic wave propagation, model accuracy has been demonstrated by comparison of phase velocity spectra with exact and/or experimental data. Accuracy superior to existing theories has been observed, as well as first order model applicability down to wavelengths on the order of typical composite microdimensions (when the energy

is partioned primarily in the first mode). In addition, a number of transient pulse cases have been treated; these exhibit good correlation with exact and/or experimental data. A sampling of typical transient pulse results for both laminated and unidirectional fibrous composites is illustrated in Figs. 1-4 of Appendix I. Typical transient wave propagation results for a complex, advanced, three-dimensional composite are given in Figs. 8-10 of Appendix I. Complete details, including extensive phase-velocity-spectra-calculations, can be found in the appropriate references listed under Section 2.3.

In the case of large deformations and elastic-plastic wave propagation, theoretical transient pulse-results for propagation parallel to the fibers of a unidirectional fibrous composite have been compared with data from a 2D-Lagrangian finite difference-code (CRAM); the latter is essentially exact. As can be observed from Appendix I, Figs. 11-14, the agreement between "exact" and approximate calculations was found to be excellent.

Model accuracy in the case of interface debonding has, to-date, been assessed by comparison with experimental data on delaminated plates composed of alternating layers of Polymethyl Methacrylate (PMMA, Rohm and Haas Type A), and 6061-T6 aluminum. The laminae of the composite were oriented perpendicular to the impact plane, and struck by a projectile fired from a 10 cm bore light gas gun. On the basis of averaged particle velocity measured at the rear face of the specimen, the model hypothesized yields excellent correlation with the experimental

results. The test setup and typical results are illustrated in Figs. 15-18 of Appendix I.

In addition to the above, studies concerning the accuracy of the thermal-portion of the continuum models were undertaken. In particular, diffusion-type processes in a laminated composite with periodic microstructure were examined. Solutions for the lowest-order models were compared with "exact" results from a finite difference code. For most cases the lowest-order "effective conductivity" theory was found to yield good results. For exceptional problems requiring a higher-order theory, a modified version of the lowest-order theory was found to yield excellent correlation between exact and approximate solutions. For many problems of the diffusion-type, these elementary equations may offer an attractive alternative to other means for obtaining solutions. Typical results for the case of heat propagating normal to the layers of the laminated composite of Fig. 1, Appendix I, are illustrated in Figs. 19 and 20 of Appendix I. In each case a uniform temperature T_o is applied to $y = 0$ from $t = 0$ and $t = t_o$ while the boundary temperature is zero for all other time. (Here $\Delta = h_1 + h_2$, $\rho_\alpha c_\alpha$ = heat capacity of α-material, k_α = thermal diffusivity). It is emphasized here that, although Figs. 19, 20 refer to a one-dimensional example, the theory is valid for three-dimensional problems. The one-dimensional case was selected mainly because the most severe test of the theory occurs when heat flow is

normal to the laminates (since material properties are discontinuous in this direction).

Finally, it is noted that a major development in theoretical modeling was effected during the previous research period. This development allows treatment of arbitrary fiber geometry and arrays. Basically the task of constructing mixture theories has been partioned into two isolated steps. The first step involves the determination of the general mixture equations for a particular problem class; these equations involve coefficients which must be determined from the detailed microstructural geometry, interface data, and constitutive relations. The second step defines the constants via a quasi-static "microboundary value problem" (MVP). Resolution of the MVP is carried out by a variational-based finite element method. The procedure has been applied to diffusion and wave propagation in unidirectional composites. Here important information has been obtained regarding the accuracy of the concentric cylinders approximation used frequently in practice for circular fibers in a hexagonal array and for rectangular fibers in a similar array. Extension of the procedure to arbitrary three dimensional geometries is under development.

A discussion of the above subject matter can be found in the survey paper listed under Section 2.3. For the readers convenience, the latter is included as Appendix II of this report.

2.2 Research Applications

The fundamental concepts embodied in the aforementioned wave propagation studies have been successfully employed in an applied research effort to model 1-D (FMI COMRAD) and AVCO 3DQP quartz pheonlic composites. These models, and the resulting numerical code (TINC) are presently in practical use by the engineering profession. Typical results for 3 DQP are illustrated in Figs. 5 - 10 of Appendix I.

2.3 List of Publications

The following publications are representative of the research progress attained during previous and present Grant periods. All publications listed were either totally or partially supported by AFOSR.

Wave Propagation

Hegemier, G.A., "Finite-amplitude Elastic-plastic Wave Propagation in Laminated Composites," J. Appl. Phys. 45: 4248-4253, 1974.
(AFOSR Technical Report No. 74-0177).

Hegemier, G.A., and G. A. Gurtman, "Finite-amplitude Elastic-plastic Wave Propagation in Fiber-reinforced Composites," J. Appl. Phys. 45:4254-4261, 1974.
(AFOSR Technical Report No. 74-0598).

Hegemier, G.A., and G. A. Gurtman, "A Mixture Theory for Wave Guide-type Propagation and Debonding in Laminated Composites," Int. J. Solids Structures 11:973-984, 1975.
(AFOSR credit line).

Hegemier, G. A., and T. C. Bache, "A General Continuum Theory with Microstructure for Wave Propagation in Elastic Laminated Composites," J. Appl. Mech. 41:101-105, 1974. (AFOSR Technical Report No. 73-1083).

Hegemier, G. A., and Adnan H. Nayfeh, "A Continuum Theory for Wave Propagation in Laminated Composites - Case 1: Propagation Normal to the Laminates," J. Appl. Mech. 40: 503-510, 1973.
(AFOSR Technical Report No. 72-0030).

Hegemier, G. A., and T. C. Bache, "A Continuum Theory for Wave Propagation in Laminated Composites - Case 2: Propagation Parallel to the Laminated," J. Elasticity 4:111-116, 1973.
(AFOSR Technical Report No. 73-2012).

Hegemier, G. A., "On a Theory of Interacting Continua for Wave Propagation in Composites," Dynamics of Composite Materials, ASME, pp. 70-121, 1972.

Hegemier, G. A., G. A. Gurtman and Adnan H. Nayfeh, "A Continuum Mixture Theory of Wave Propagation in Laminated Fiber Reinforced Composites," Int. J. Solids Structures 9: 3945-415, 1973.

Hegemier, G. A., and T. C. Bache, "A General Continuum Theory for Viscoelastic Laminated Composites."
(AFOSR Technical Report 74-0135).

Bache, T. C., and G. A. Hegemier, "On Higher-order Elasto-dynamic Plate Theories," J. Appl. Mech. 41:423-429, 1974.

Nayfeh, Adnan H., "Time Harmonic Waves Propagating Normal to the Layers of a Multi-layered Periodic Media," J. Appl. Mech. 41:92-96, 1974.

Felix, M. P., "Attenuation and Dispersion Characteristics of Various Plastics in the Frequency Range 1-10 MHz," J. Composite Materials 8:275-287, 1974.
(AFOSR Technical Report No. 74-0888).

Nemat-Nasser, S., "General Variational Methods for Waves in Elastic Composites," J. Elasticity 2:73-90, 1972.
(AFOSR Technical Report No. 72-0321).

Nemat-Nasser, S., "Harmonic Waves in Layered Composites," J. Appl. Mech. 39:850-852, 1972.
(AFOSR credit line).

Felix, M. P., "Short Duration Stress Pulse Propagation in Solids and Liquids," Ph. D. Dissertation, University of California, San Diego, 1973.

Nayfeh, Adnan H., "A Continuum Mixture Theory of Heat Conduction in Laminated Composites," J. Appl. Mech., Paper No. 75-APMW-31, 1975.
(AFOSR credit line).

Nayfeh, Adnan H., "Asymptotic Behavior of Eigenvalues for Finite Inhomogeneous Elastic Rods," J. Appl. Mech. 39: 595-597, 1972.
(AFOSR credit line).

Bache, T. C., "A Continuum Theory with Microstructure for Wave Propagation in Composite Materials," Ph. D. Dissertation, University of California, San Diego, 1973.

Nemat-Nasser, S., "General Variational Principles in Nonlinear and Linear Elasticity with Applications," Mechanics Today 1:214-261, 1972.
(AFOSR credit line).

Felix, M. P., and A. T. Ellis, "Stress Pulse Propagation in Solids: A Closer Look at Dispersion," Appl. Phys. Ltrs. 21:532-534, 1972.
(AFOSR Technical Report No. 73-1952).

Murakami, H., A. Maewal, and G. A. Hegemier, "Mixture Theory for Longitudinal Wave Propagation in Unidirectional Composites with Cylindrical Fibers of Arbitrary Cross-Section, I: Formulation," to be submitted for publication.

Murakami, H., A. Maewal, and G. A. Hegemier, "Mixture Theory for Longitudinal Wave Propagation in Unidirectional Composites with Cylindrical Fibers of Arbitrary Cross-Section, II: Computational Procedure," to be submitted for publication.

Diffusion

Maewal, A., T. C. Bache, and G. A. Hegemier, "A Continuum Model for Diffusion in Laminated Composite Media,: J. Heat Transfer 98:133-138, 1976.
(AFOSR credit line).

Maewal, A., G. A. Gurtman, and G. A. Hegemier, "A Mixture Theory for Quasi-One-Dimensional Diffusion in Fiber-Reinforced Composites," to appear in J. Heat Transfer, 1977.
(AFOSR credit line).

Murakami, H., G. A. Hegemier, A. Maewal, "A Mixture Theory for Thermal Diffusion in Unidirectional Composites with Cylindrical Fibers of Arbitrary Cross Section," submitted to J. Solids Structures, 1977.
(AFOSR credit line).

Mechanics of Failure

Ashbaugh, N. E., "Stresses in Laminated Composites Containing a Broken Layer - Part I: Analysis," J. Appl. Mech. 40: 533-540, 1973.
(AFOSR Technical Report No. 73-0032).

Asbaugh, N. E., "Stresses in Laminated Composites Containing a Broken Layer - Part II; Numerical Results", J. Appl. Mech. 40:533-540, 1973.
(AFOSR Technical Report No. 72-0031).

Asbaugh, N. E., "On the Opening of a Finite Crack Normal to an Interface," J. Appl. Mech. 40:626-628, 1973.
(AFOSR Technical Report No. 72-1192).

Ashbaugh, N. E., "The Stress Field Around a Broken Layer in a Composite Material", Ph. D. Dissertation, University of California, San Diego, 1971.

Lanier, Y. N., and Y. C. Fung, "Fiber Composite Columns under Compression," J. Composite Materials 6:387-401, 1972.
(AFOSR Technical Report No. 71-3029).

Acoustic Holography

Felix, M. P., "Laser-generated Ultrasonic Beams," Review Science Instrumentation 45:1106-1108, 1974.
(AFOSR Technical Report No. 74-1043).

Ellis, A. T., and M. P. Felix, "Laser-induced Stress in Materials," Invited paper Proc. Society of Photo-Optical Instrumentation Engineers: Developments in Laser Technology II (San Diego, Calif.), Vol. II, pp. 199-202, Aug. 1973.
(AFOSR credit line)

Felix, M. P., and A. T. Ellis, "Laser-induced Liquid Breakdown -A Step- by-Step Account," Appl. Phys. Ltrs. 19:484-486, 1971.
(AFOSR credit line).

Felix, M. P., and W. Nachbar, "A Closer Look at Laser Damage in PMMA," Appl. Phys. Ltrs. 25:25-27, 1974.
(AFOSR credit line).

Structural Optimization (Minimum Weight Design)

Hegemier, G. A., and H. T. Tang, "A Variational Principle, the Finite Element Method, and Optimal Structural Deisgn for Given Deflection," Proc. Symposium on Optimization in Structural Design (eds: A. Sawezuk, Z. Mróz), IUTAM Symposium (Warsaw, Poland, 1973), Springer-Verlag, N. Y., pp. 464-483, 1975.
(AFOSR Technical Report No. 74-0151).

Hegemier, G. A., "Application of the Direct Method of Liapunov to a Class of Cylindrical Shell Dynamic Stability Problems," Proc. Symposium on This Shell Structures, 1973 (eds: Y. C. Fung and E. E. Sechler), Prentice-Hall, Inc., Part II, Chapter 5, 1974.

Survey Papers

Hegemier, G. A., "Mixture Theories with Microstructure for Wave Propagation in Diffusion in Composite Materials," Proc. Symposium on Continuum Models of Discrete Systems (ed: J. Provan), June 26-July 2, 1977, Montreal, Quebeck, Canada.
(AFOSR credit line).

Dynamical Theories of Composite Rods

Hegemier, G. A., and S. Nair, "A Nonlinear Dynamical Theory for Heterogeneous, Anisotropic, Elastic Rods," AIAA Journal 15:8-15, 1977.
(AFOSR credit line).

Nair, S., and G. A. Hegemier, "Effect of Initial Stresses on the Small Deformations of a Composite Rod," submitted to AIAA Journal.

APPENDIX I

Compendium of Typical Theoretical Results

Presented in this Appendix is a sampling of typical transient pulse and diffusion calculations carried out using the Theory of Interacting Continua (TINC). The cases discussed include laminated and unidirectional fibrous composites as well as a complex 3-dimensional layup. Results of the TINC theory for each example are compared to experimental data.

Laminated Composites

The geometry of the laminated composites studies is illustrated in Fig. 1. One problem of interest is that of symmetric (P) wave propagation parallel to the layers, with material behavior restricted to the linear elastic range. A comparison of TINC and experimental results is given in Fig. 2. The experimental results were reported by Whittier and Peck [1] for specimens composed of Thornel (high modulus carbon) fibers reinforcing a carbon phenolic matrix. Specimens of 1/4-inch thickness were subjected to a uniform pressure at the left boundary, with a step function time-dependence induced by a gas dynamic shock wave of about 70 psi. The numerical calculations were initiated by impacting a step function velocity of 7.786 cm/sec to both constituents at the boundary. While this condition does not correspond precisely to the experiment, it was felt that the error introduced would be negligible when far removed

from the front surface. Figure 2 depicts the comparison between experiment and theoretical results for averaged rear surface velocity, normalized on the boundary input velocity. Since absolute times were not measured in the tests, theoretical and experimental results were matched at their respective first peak arrivals. In the figure, results from the full TINC equations solved numerically are denoted "Continuum mixture theory." The results denoted "Simplified theory" are for an elementary form of the TINC theory admitting a closed-form solution.

Unidirectional Fibrous Composite

The TINC theory has been applied to the problem of wave propagation parallel to the fibers of a unidirectionally reinforced composite with hexagonal array. The hexagonal array is approximated by concentric, linearly elastic cylinders as illustrated in Fig. 3.

In Fig. 4, transient pulse data predicted by TINC is compared with experimental data on a unidirectional quartz phenolic fibrous composite. The experiments were subjected to a 70 psi step function in pressure via a shock tube. The figure depicts the comparison between the experimental and TINC theory code predictions of area-averaged rear surface velocity. Results of the simplified TINC theory are also portrayed. Once again the experimental and theoretical results are matched at their first peak arrivals since absolute arrival times were not measured experimentally. As was the case in Fig. 2, the times shown are those

predicted by the theory.

Three-dimensional Layups

Predictions of transient pulse behavior from the TINC theory have been compared to experimental results for a 3-dimensional quartz phenolic composite (3DQP) manufactured by AVCO. A representative selection of the results are given here.

A "block" 3DQP specimen (Fig. 5) was subjected to shock tube tests by the Aerospace Corporation. The test procedure is the same as that used for laminated and fibrous composites and is described above. Once again the theoretical and experimental boundary conditions are not identical, but this decrepancy is expected to introduce little error. The averaged rear surface velocity measured by experiment is compared to that predicted by the TINC theory in Fig. 6. Also shown are results predicted by the elementary "Head of the Pulse" approximate [2]. The experimental data has been forced to coincide with the theoretical at $V/V_o = 1/3$ since absolute arrival times were not measured.

Another set of relatively low pressure wave propagation experiments were performed at the Air Force Weapons Laboratory using a light gas gun and "midspace" 3DQP specimens, shown in Fig. 7. In this test, three specimens of different thicknesses were mounted on a single target and impacted with a .01-inch mylar flyer. The input stress profiles for the three specimens are illustrated in Fig. 8. For the TINC calculations,

input velocity time-histories corresponding to the stress-time data of Fig. 8 were used. A comparison of experimental and theoretical results for the thickest of these specimens is shown in Fig. 9. Since absolute arrival times were not measured, the two curves are forced to coincide at their peak pressures. The agreement here is excellent, especially in view of the fact that the wave is measured only 2-1/2 microdimensions from the front surface. Also, with the 10kb input stress, this is a nonlinear calculation.

The AFWL also performed a series of high-pressure gas gun experiments on "midspace" 3DQP specimens (Fig. 7). Experimental and theoretical data are compared in Fig. 10. The observed agreement indicates that the thermodynamic and nonlinear constitutive behavior incorporated into the TINC theoretical model are adequate. Note that here the rear surface velocity is measured only 1-1/2 microdimensions from the front surface. Thus, as before, the TINC theory, though derived as an "outer" solution, yields surprisingly good results even at locations quite near the boundary.

Comparison of TINC and 2-D Finite Difference Code

It is of interest to compare the results from a TINC calculation to those of a typical two-dimensional Lagrangian finite difference code which is essentially exact. Such a code (CRAM) is available at Systems, Science and Software, Inc. The two codes were compared for the

concentric cylinder geometry of Fig. 11. Computer costs for CRAM were approximately 500 times those for running the TINC code. Several typical results are illustrated in Figs. 12-14 for a square wave input velocity (shown as problem #2 on Fig. 11). Once again, the calculations were carried out within a few microdimensions of the boundary.

Debonding of Constituent Interfaces

Model accuracy in the case of interface debonding or cracking has, to date, been assessed by comparison with experimental data dealing with delaminated plates composed of alternating layers of Polymethyl Methacrylate (PMMA, Rohm and Haas Type A), and 6061-T6 aluminum. The laminae of the composite were oriented perpendicular to the impact plane, and struck by a projectile fired from a 10 cm bore light gas gun. On the basis of averaged particle velocity measured at the rear face of the specimen, the model hypothesized yields excellent correlation with the experimental results.

The test setup employed is illustrated in Fig. 15. Typical correlation between theoretical and experimental results is shown in Figs. 16-18. Complete details can be found in reference [13].

Diffusion

The laminated geometry of Fig. 1 was selected to evaluate the continuum model construction procedure for diffusion problems (a

complete discussion of this work can be found in reference [4]). The case of heat propagation normal (in the y-direction) to the layers was selected for a comparison of exact and continuum theory solutions since it is known that this case represents the most severe test of the latter. Figure 19 represents a case of similar material properties whereas Fig. 20 illustrates the comparison for widely differing material properties. Continuum theory-results were obtained via closed-form solutions for a square-wave temperature input at the boundary y = 0. "Exact" results were obtained using a finite difference code. The calculations illustrate the ability of the first-order theory to model microstructure details and closely match the exact data.

REFERENCES

1. Whittier, J.S., and J.C. Peck, "Experiments on Dispersive Pulse Propagation in Laminated Composites and Comparison with Theory," J. Appl. Mech. 36:485-490, 1969.

2. Peck, J.C., and G.A. Gurtman, "Dispersive Pulse Propagation Parallel to the Interfaces of a Laminated Composite," J. Appl. Mech. 36:479, 1969.

3. Hegemier, G.A., and G.A. Gurtman, "A Mixture Theory for Wave Guide-Type Propagation and Debonding in Laminated Composites," Int. J. Solids Structures 11:973-984, 1975.

4. Maewal, A., T.C. Bache, and G.A. Hegemier, "A Continuum Model for Diffusion in Laminated Composite Media," J. Heat Transfer 98:133-138, 1975.

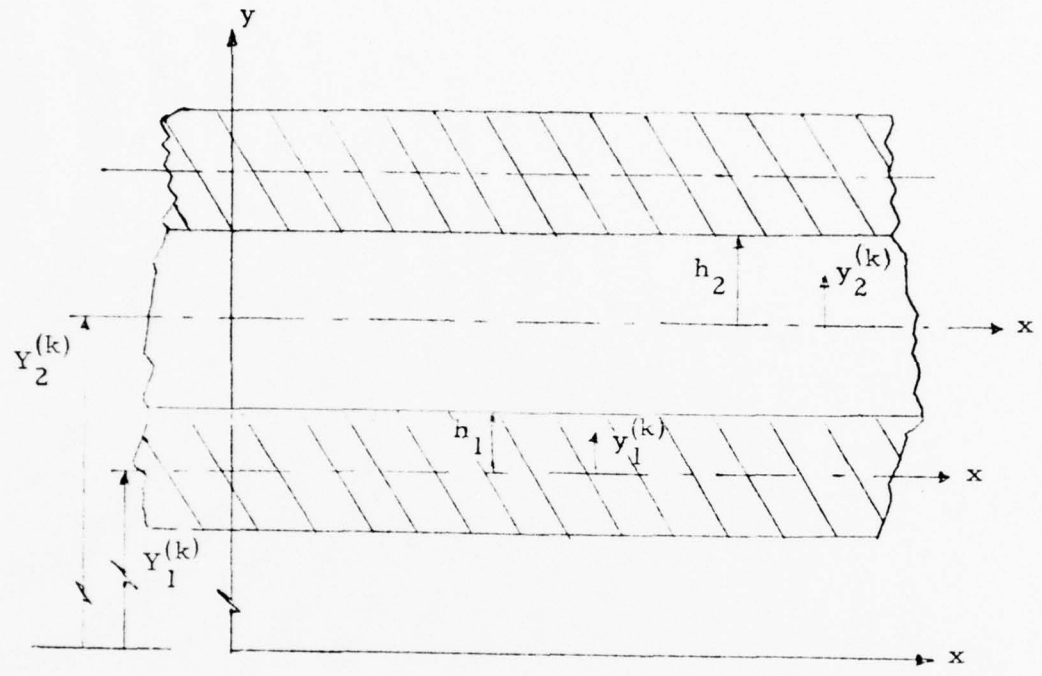

Fig. 1. Geometry and coordinate system.

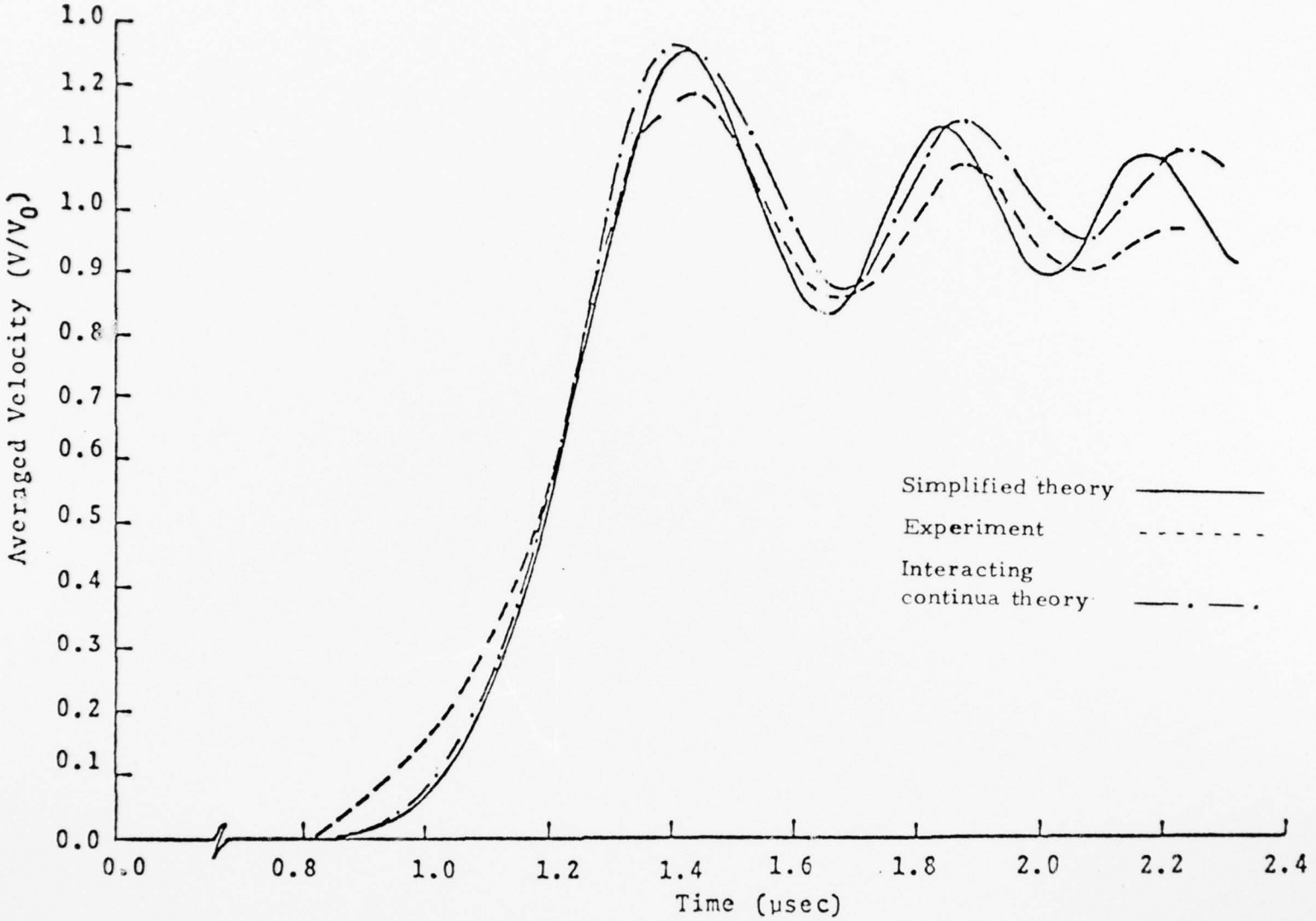

Fig. 2. Comparison of TINC and experimental rear surface velocity results for thornel reinforced carbon phenolic laminates.

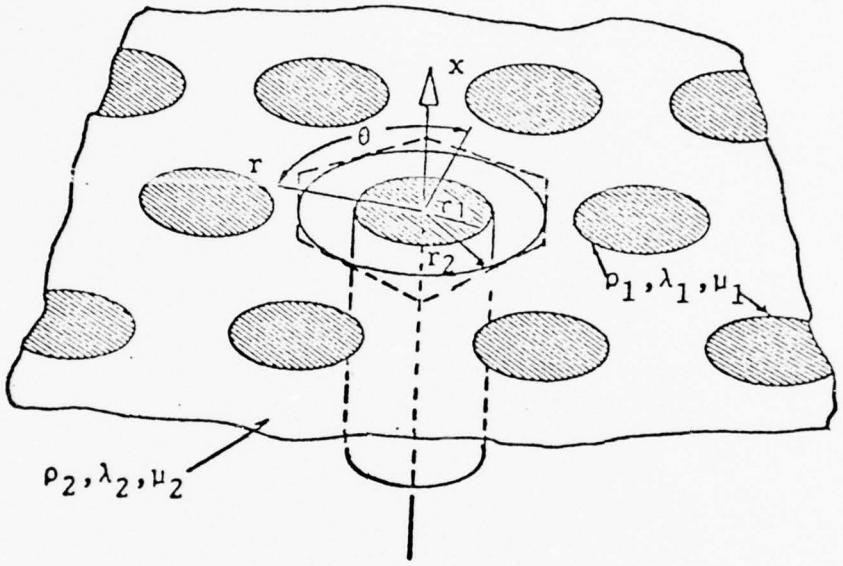

Fig. 3. Unidirectionally fiber-reinforced composite with hexagonal array.

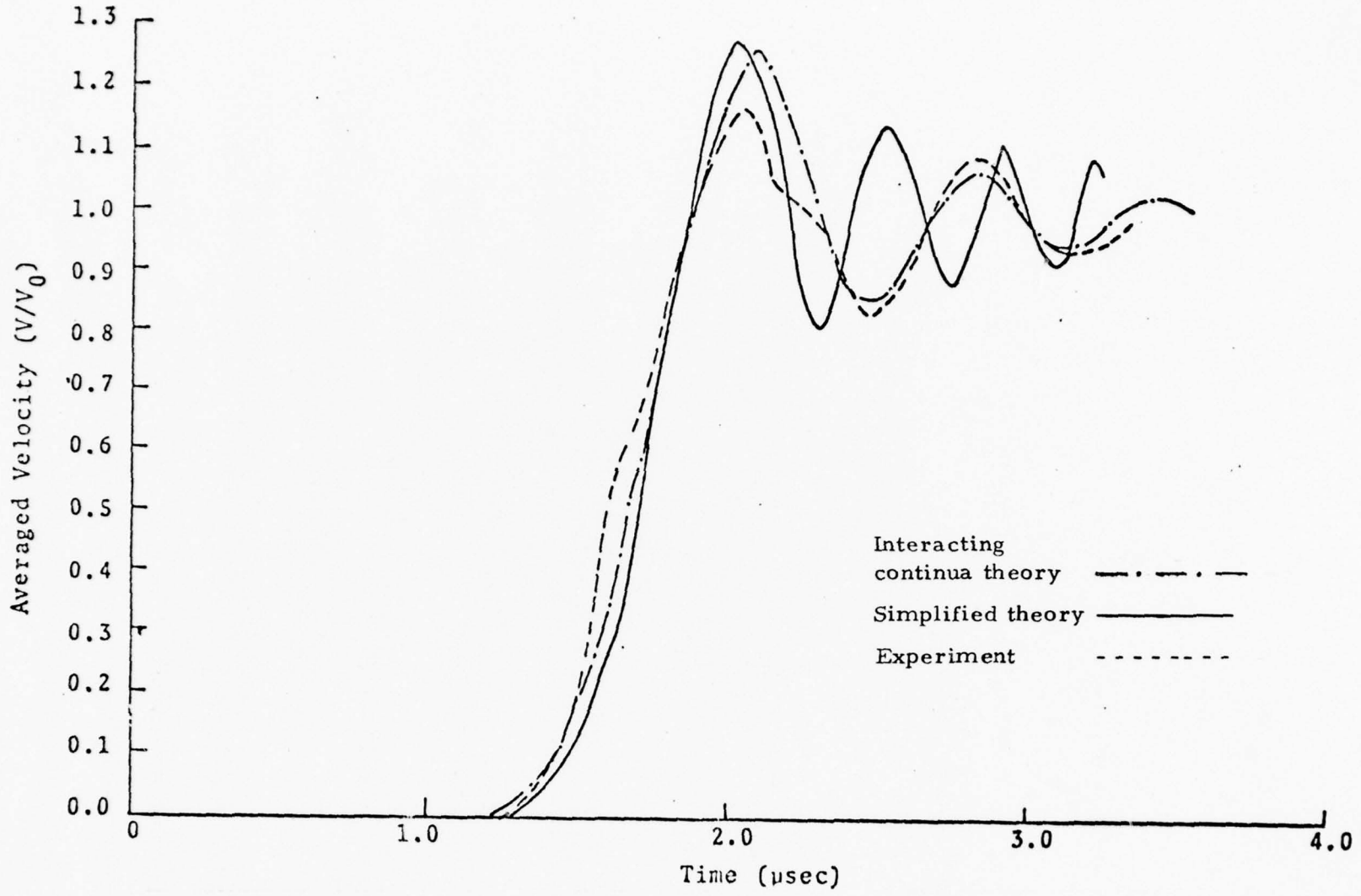

Fig. 4. Comparison of TINC and experimental rear surface velocity results from quartz fiber reinforced phenolic.

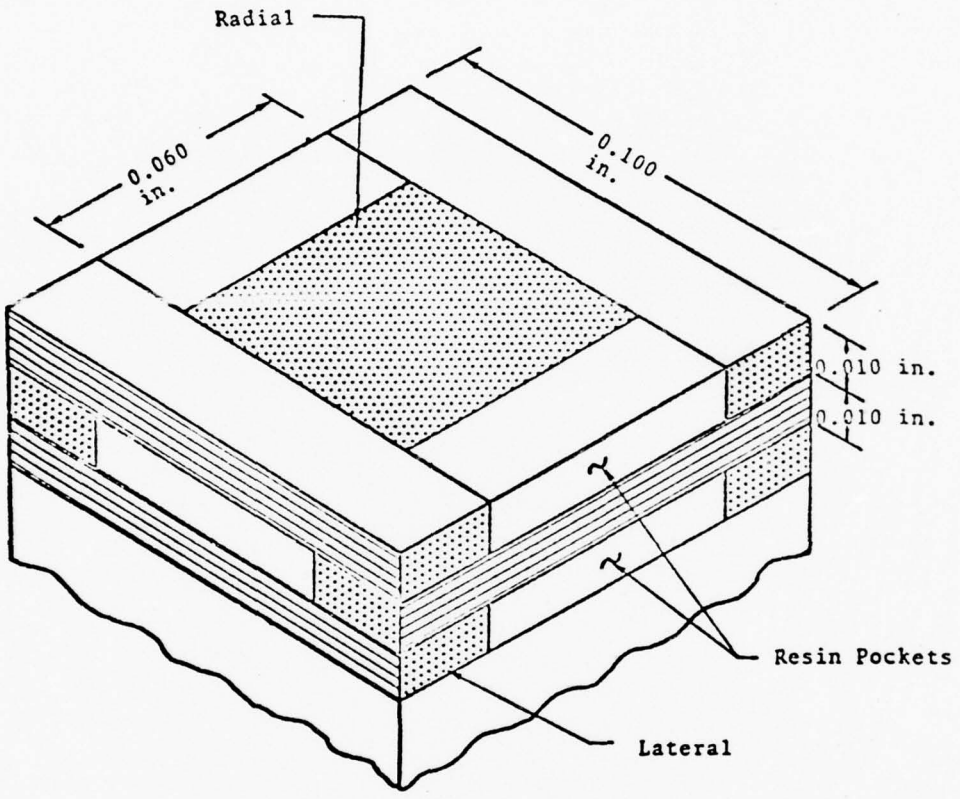

Fig. 5. AVCO 3DQP "Block" material.

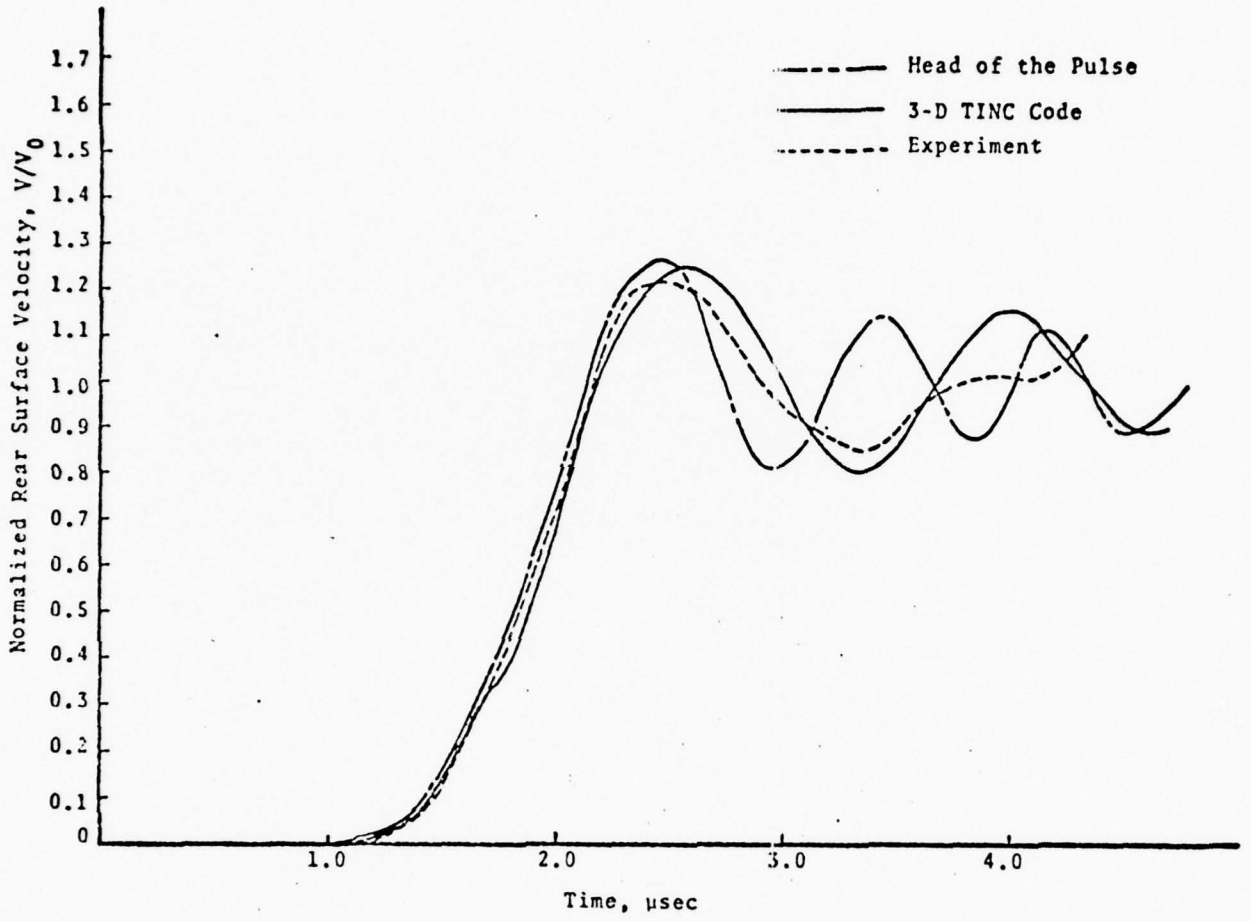

Fig. 6. Comparison of theoretical and experimental results for step pulse in "block" 3DQP (x = 0.635 cm).

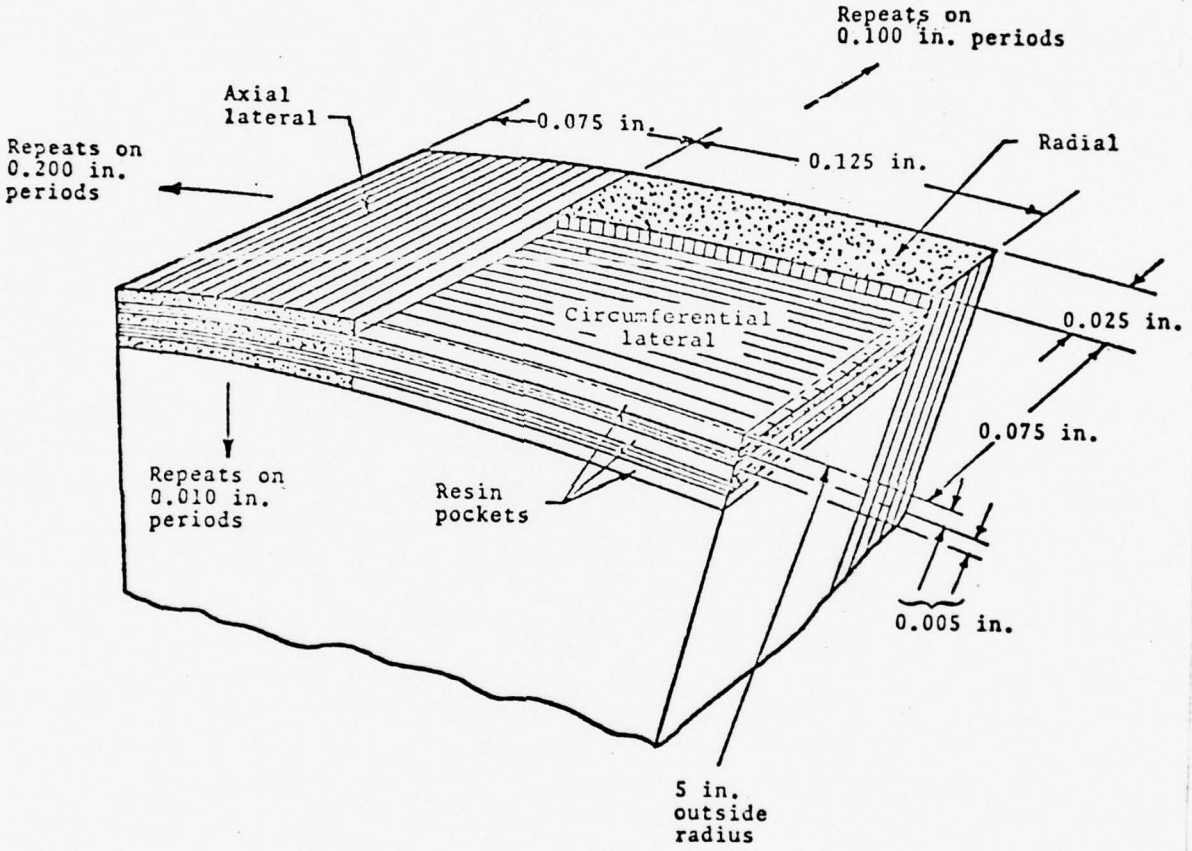

Fig. 7. AVCO 3DQP "shell" material (midspaced).

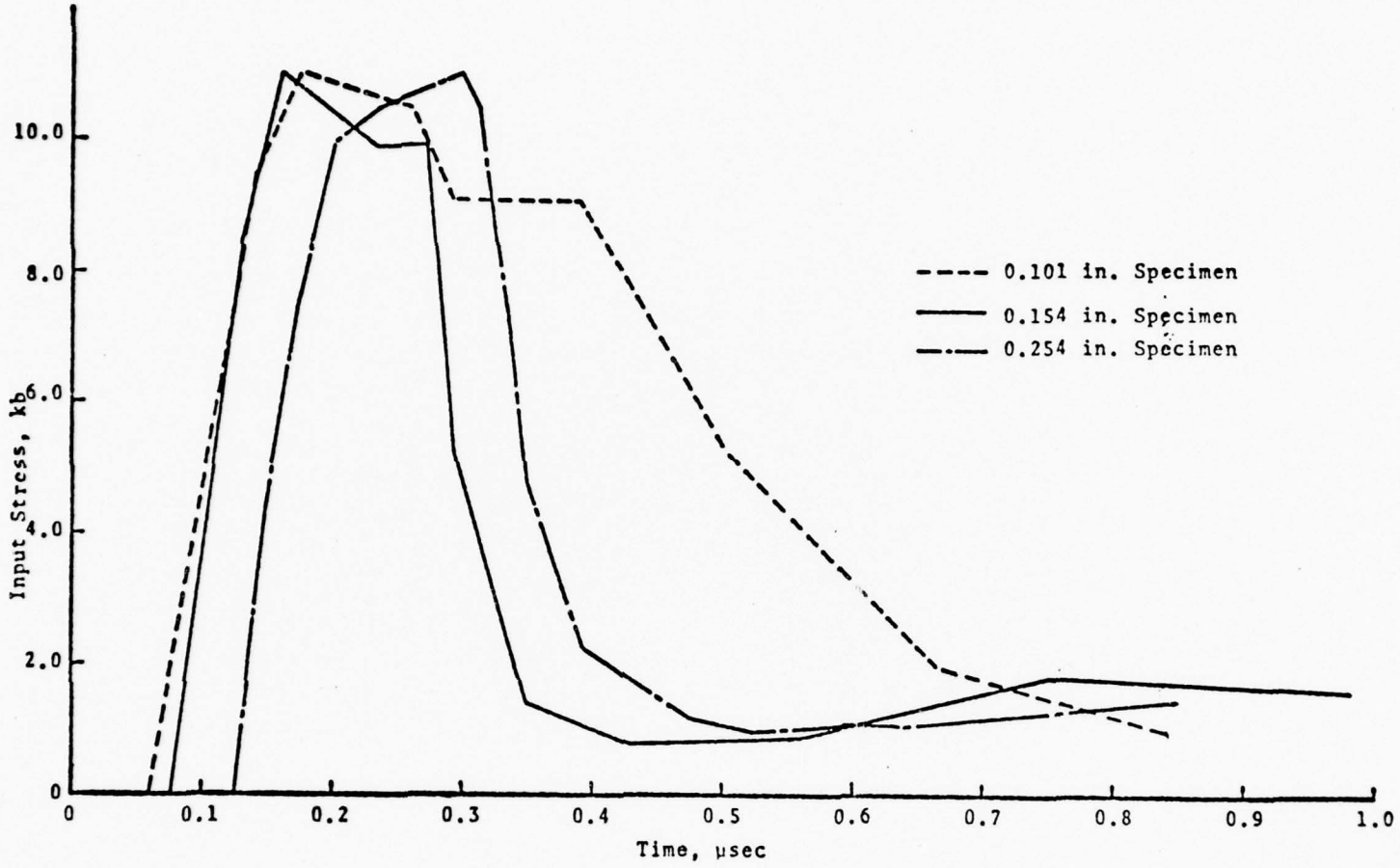

Fig. 8. Input stress profiles for AFWL shot 326.

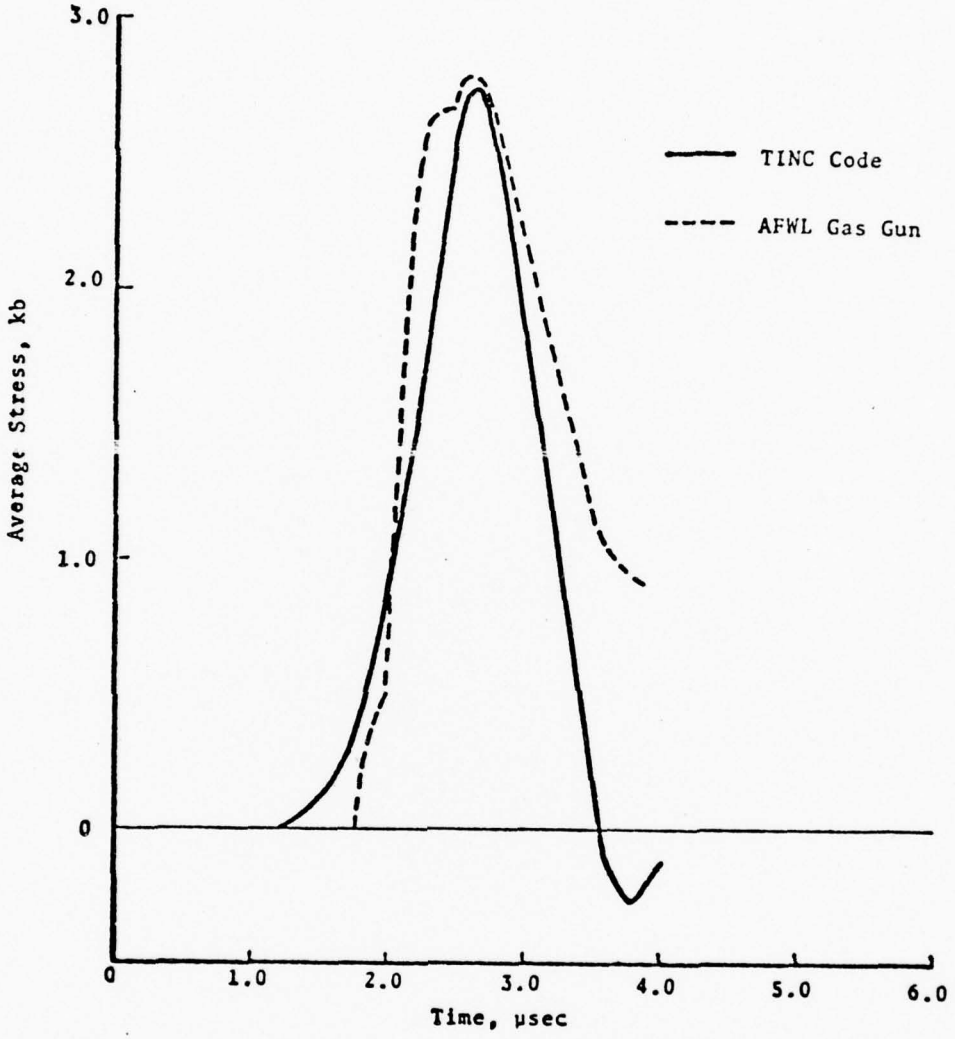

Fig. 9. Stress history at rear of 0.254 in. 3DQP plus 0.060 in. plexiglass (shot 326).

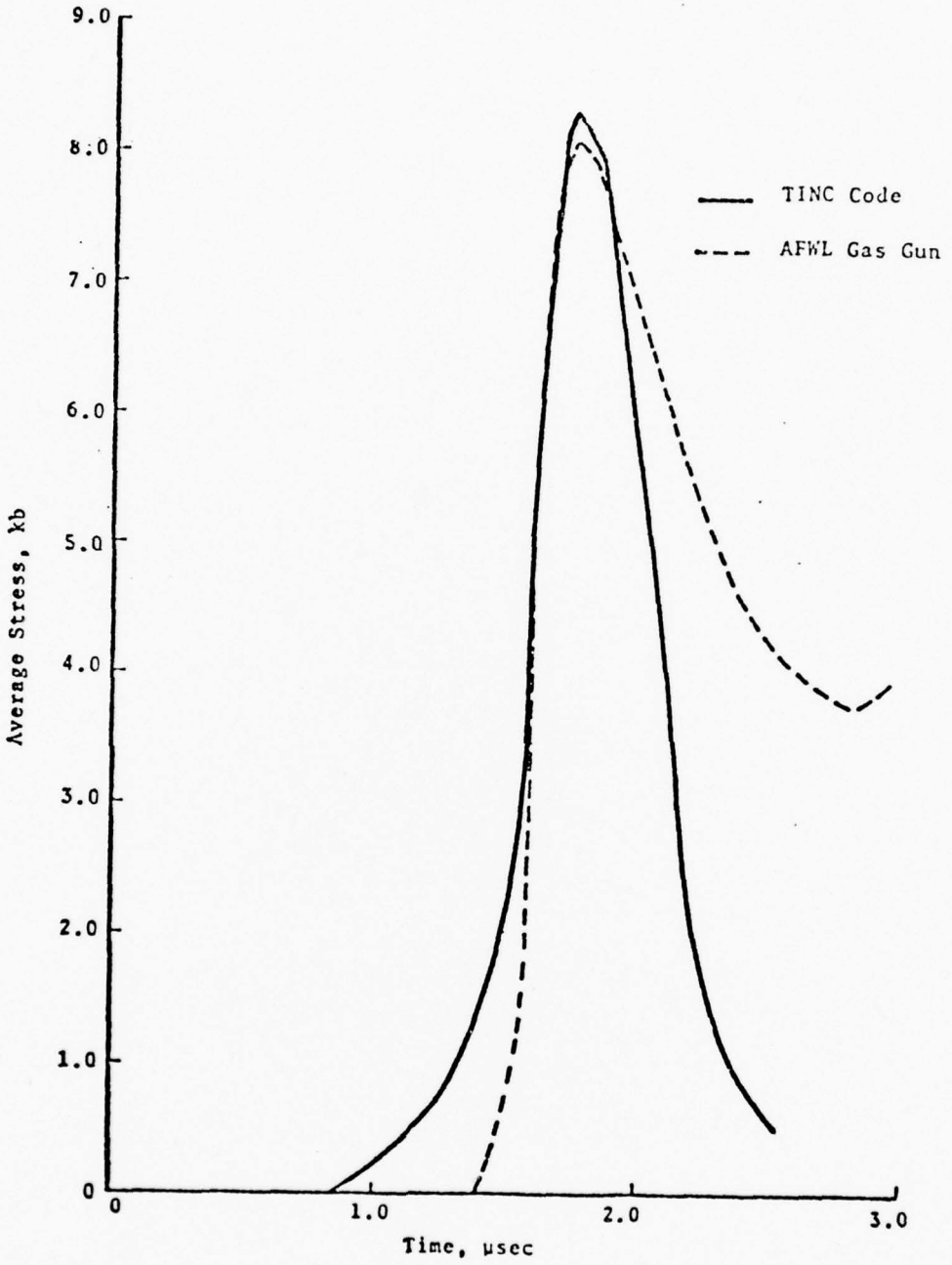

Fig. 10. Stress history at rear of 0.154 in. 3DQP plus 0.060 in. plexiglass (shot 314).

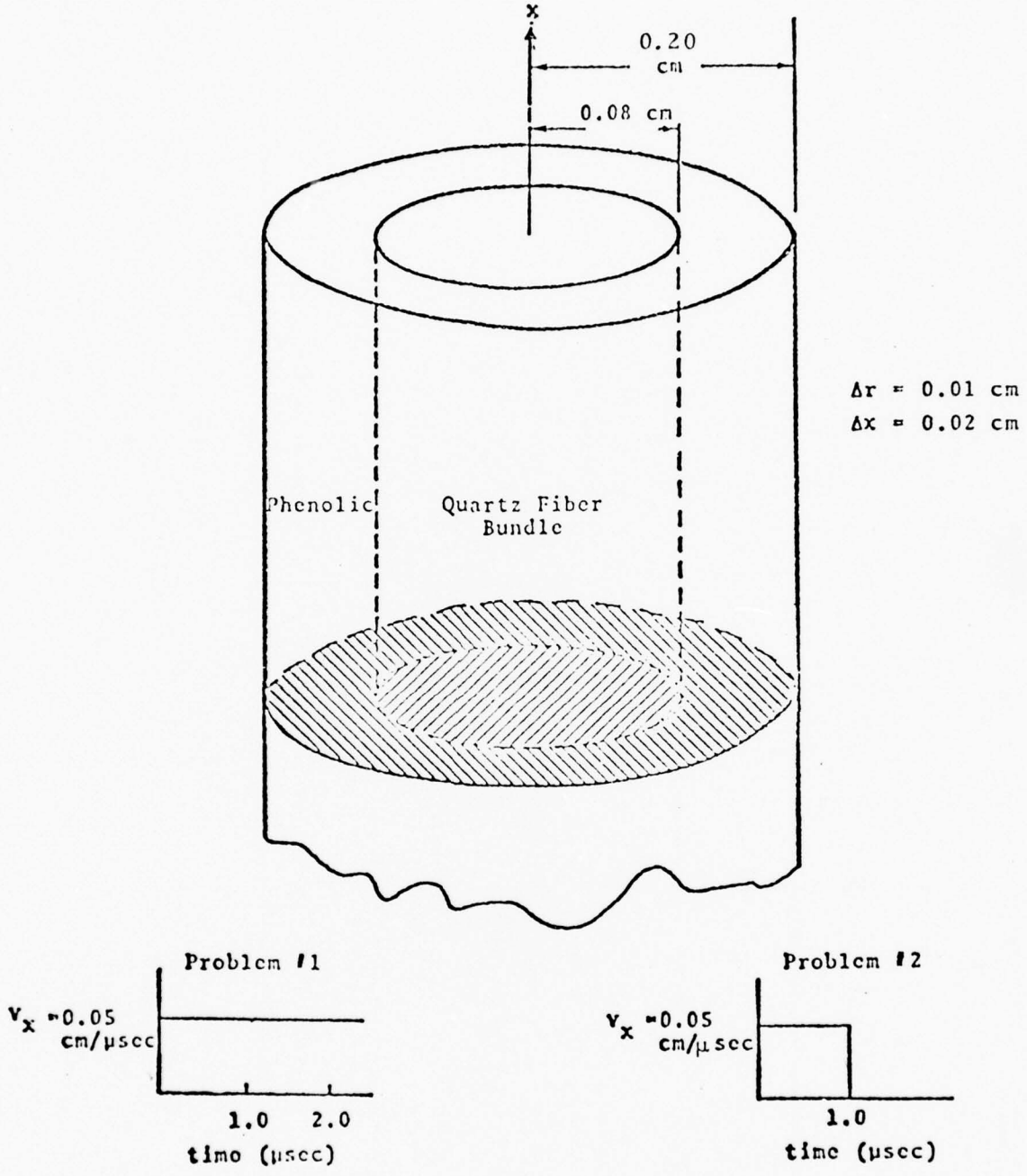

Fig. 11. Geometry for 2D CRAM Calculation.

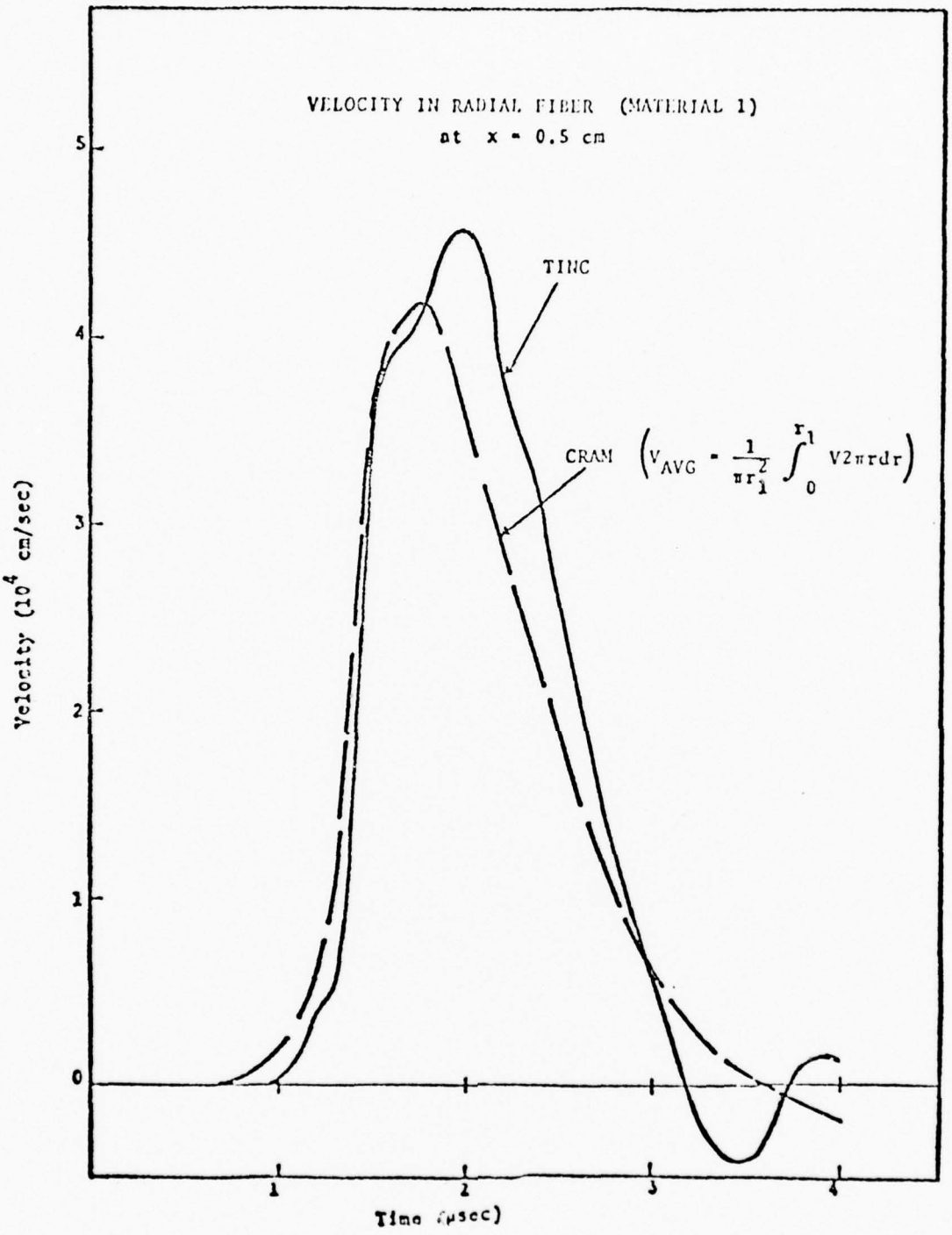

Fig. 12. Comparison of TINC and average CRAM particle velocity histories for radial fiber.

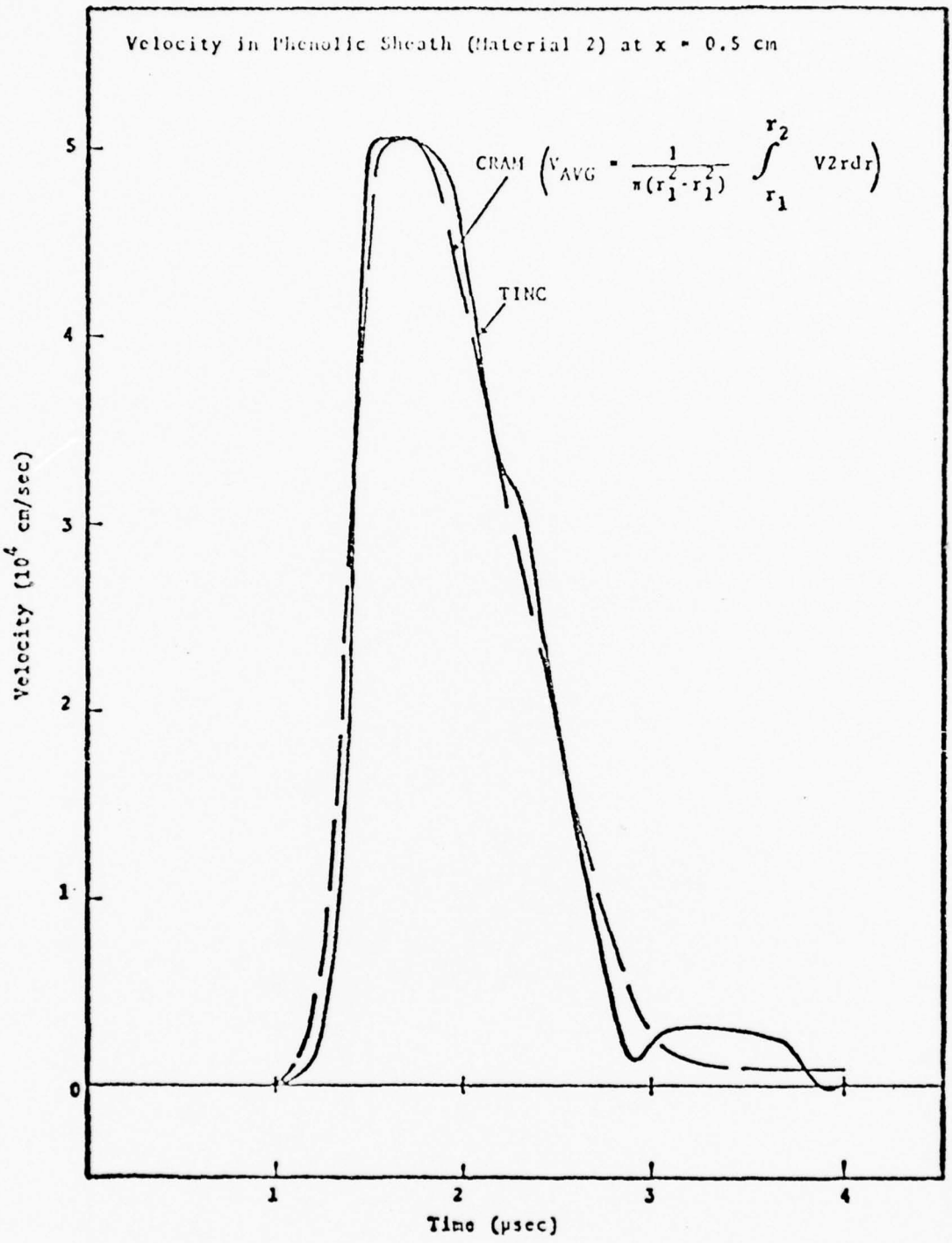

Fig. 13. Comparison of TINC and average CRAM particle velocity histories for sheath.

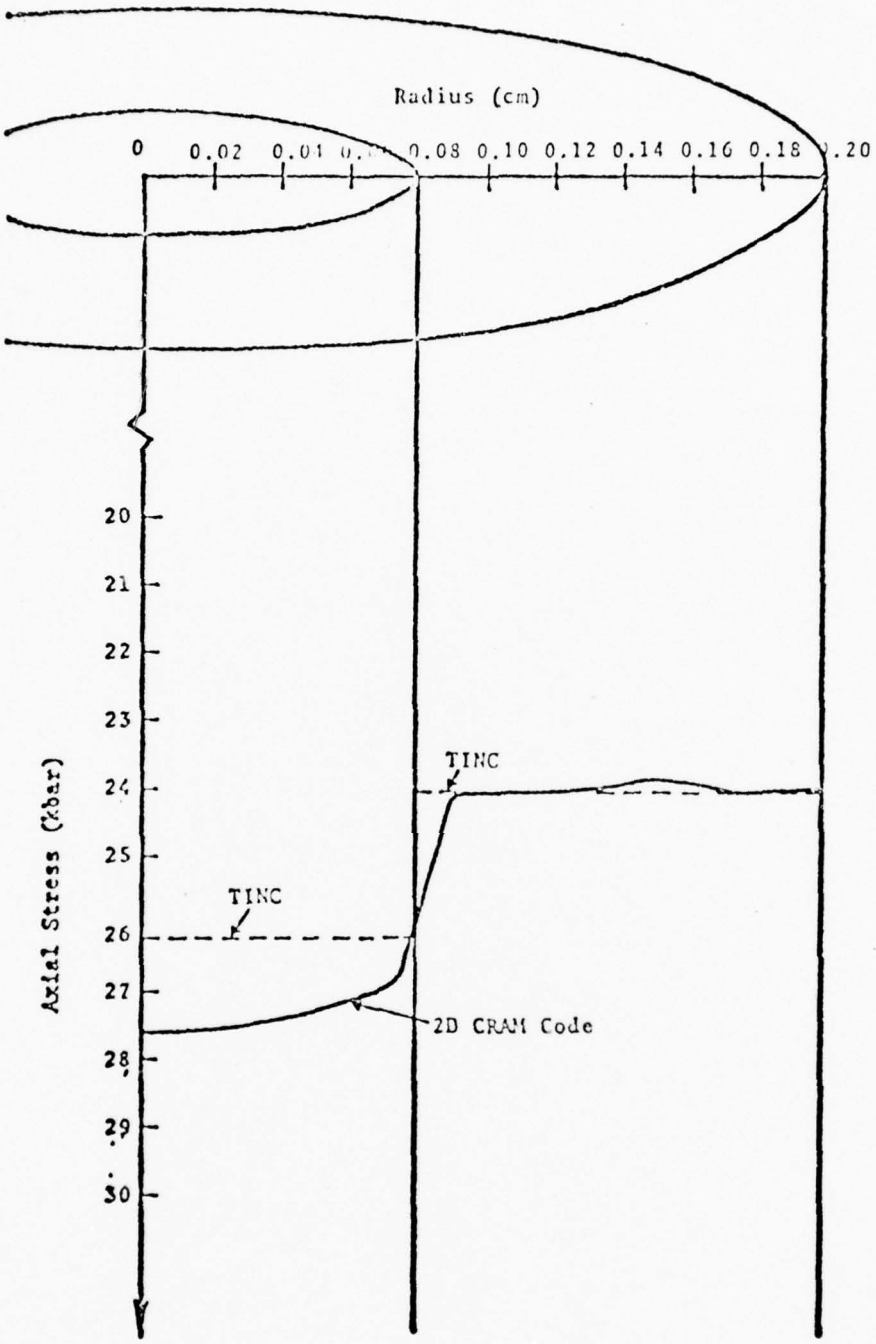

Fig. 14. Comparison of TINC and CRAM predictions of axial stress (x = 0.2 cm, t = 1.0 μsec).

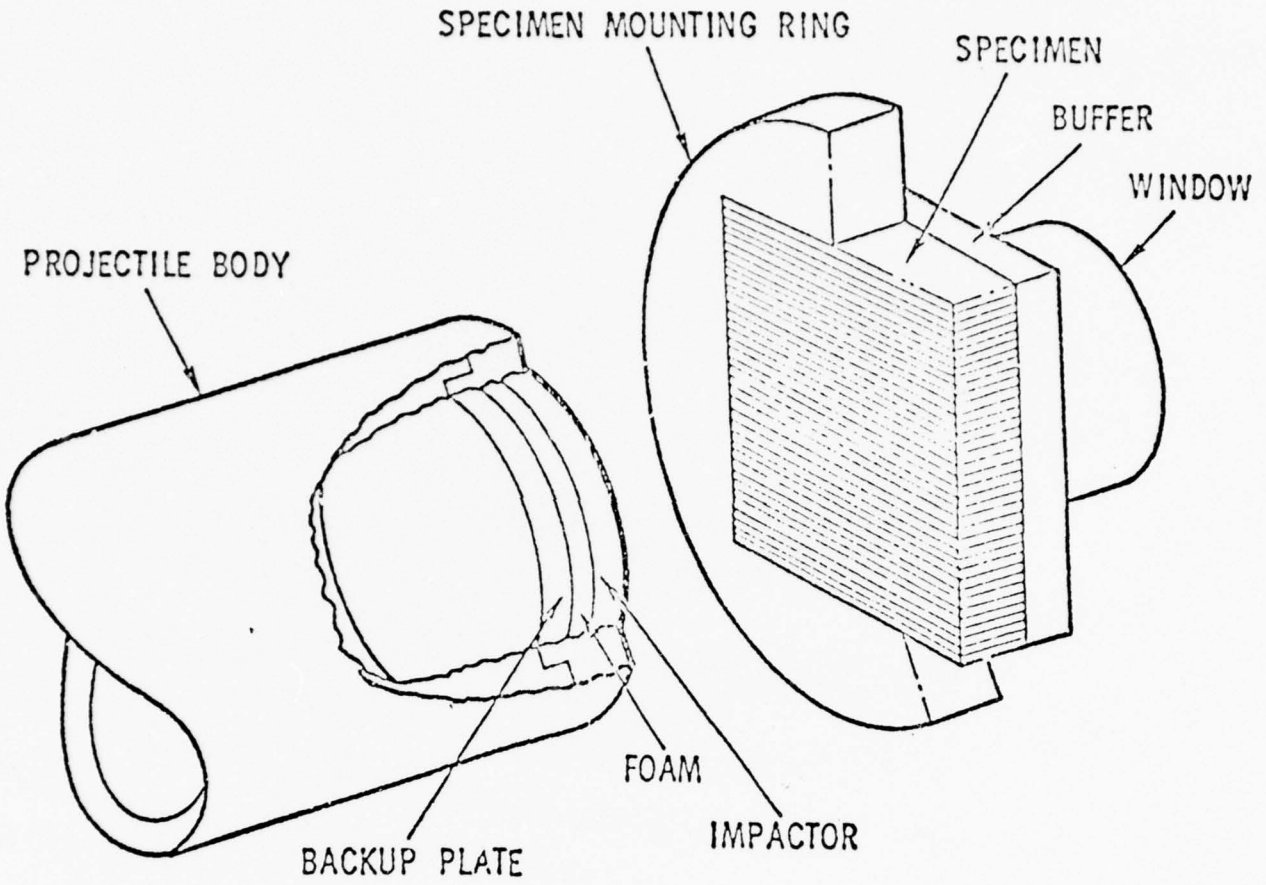

Fig. 15. Experimental arrangement for Sandia experiments.

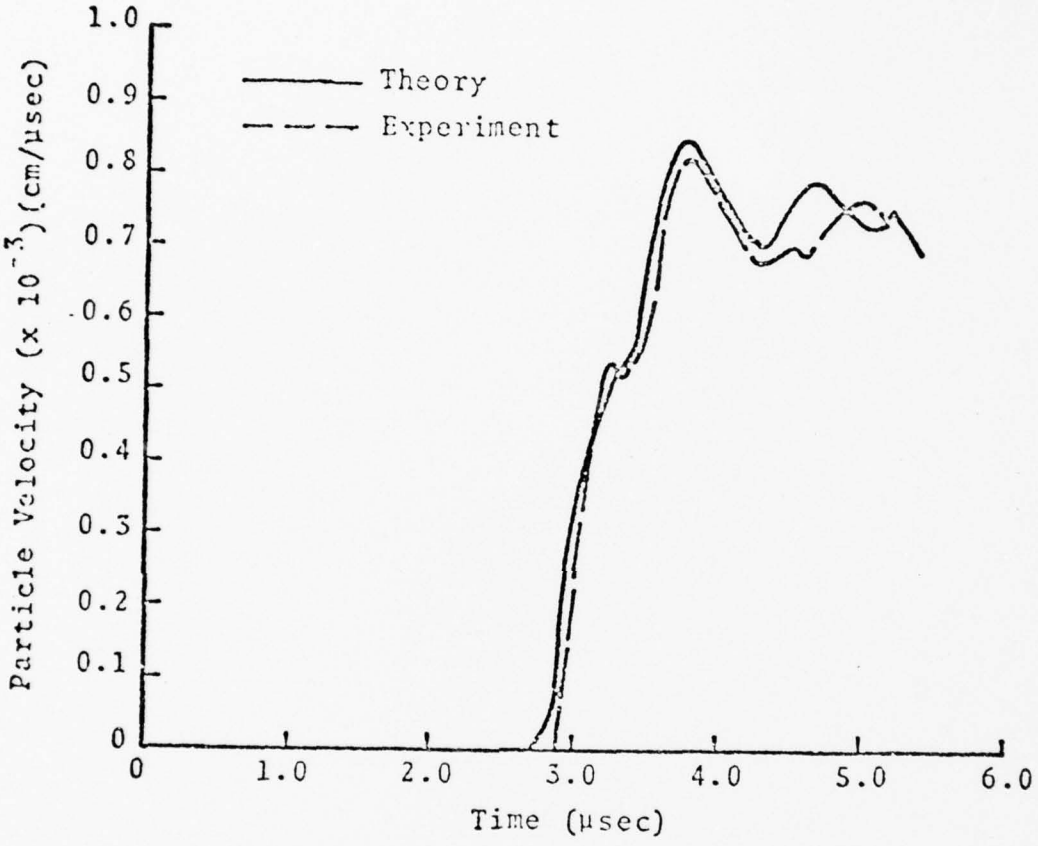

Fig. 16. Comparison of theory with experiment No. 2.

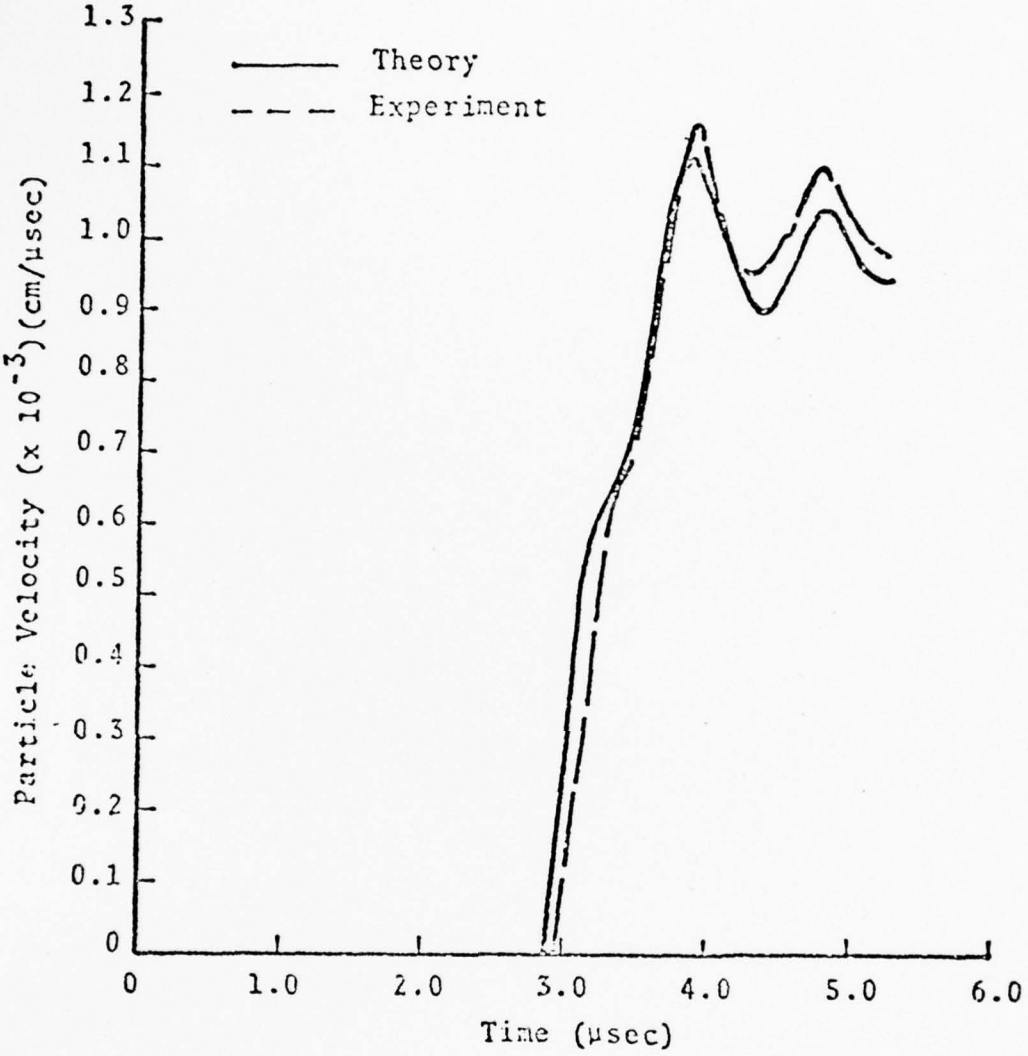

Fig. 17. Comparison of theory with experiment No. 6.

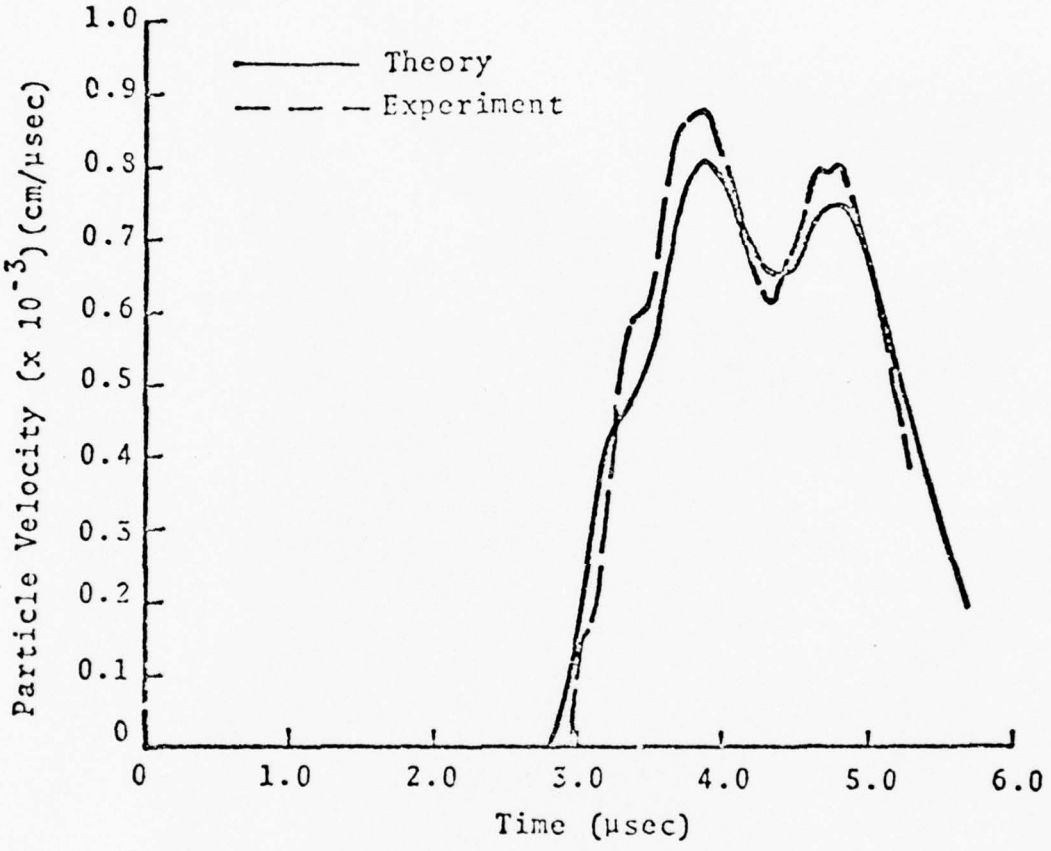

Fig. 18. Comparison of theory with experiment No. 7.

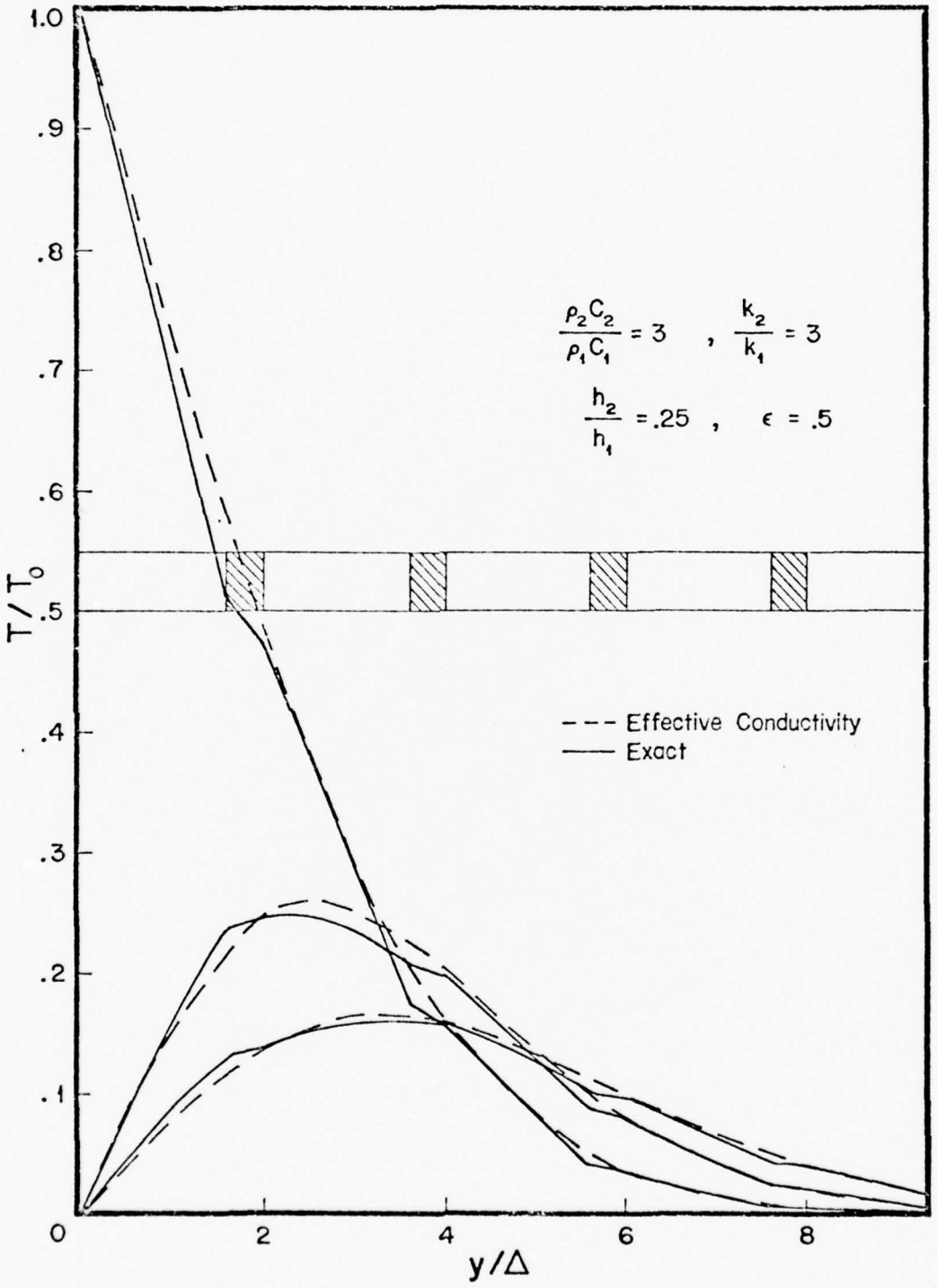

Fig. 19. Temperature distribution at τ = 1, 1.5 and 2 for similar material properties and small duration of input pulse t_o.

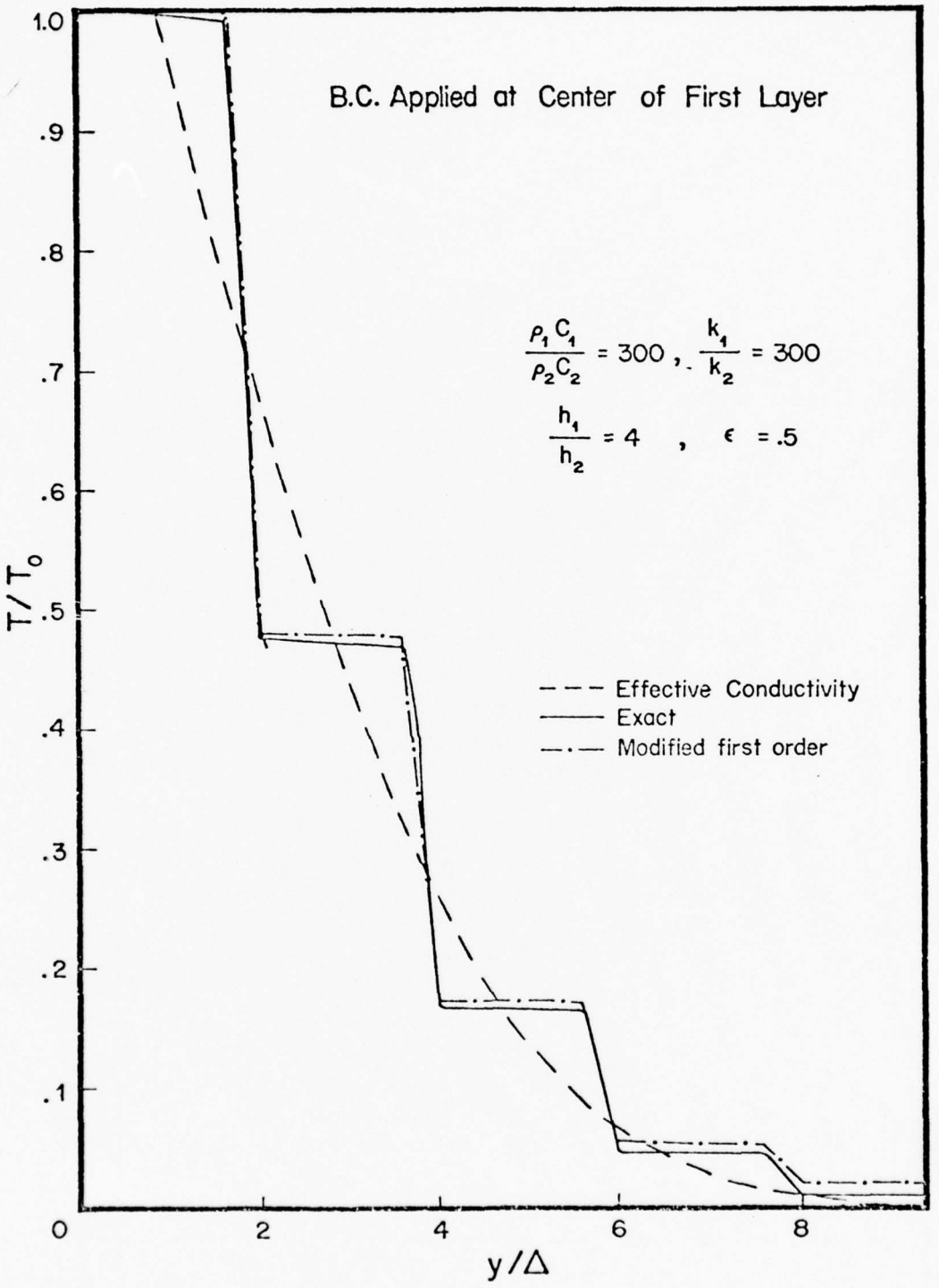

Fig. 20. Temperature distribution at $\tau = 1$ for widely differing material properties and small t_o.

APPENDIX II

MIXTURE THEORIES WITH MICROSTRUCTURE FOR WAVE PROPAGATION AND DIFFUSION IN COMPOSITE MATERIALS

Two procedures for constructing mixture theories with microstructure are discussed for wave propagation and thermal diffusion processes in binary laminated and fibrous composites. Each method proceeds from the composite microstructure and is based upon an asymptotic scheme wherein the ratio of transverse-to-longitudinal characteristic times associated with a physical process is assumed to be small. The methods retain considerable information regarding the mechanical and/or diffusive fields within the microcomponents. Theoretical results are compared with both experimental and exact data in an effort to evaluate model accuracy. The presentation includes treatment of geometric, constitutive, and interface nonlinearities.

1. INTRODUCTION

A considerable number of continuum theories have been proposed for thermomechanical processes in composites. The continuum theory of mixtures represents one of the more important and successful theoretical descriptions of such multiphase materials. According to this concept, the composite constituents are modeled, at each instant of time, as superposed continua in space. Each continuum is allowed to undergo individual deformations. The microstructure of an actual composite is then simulated by specifying the interactions between the continua.

Mixture theories for multiphase materials have been developed from both macrostructural and microstructural viewpoints. The vast majority of activity, however, has been directed toward the former, which concerns the formulation of a general theoretical framework for classes of mixtures based upon certain phenomenological postulates that avoid detailed microstructural considerations. Excellent accounts of this approach can be found in [1-3].

The development of mixture theories from the microstructural viewpoint represents a more difficult task. The reward, however, is a model - which shall be called a mixture theory with microstructure - that is completely determined by the geometry and constitutive relations of the individual components and which provides, to a certain degree of accuracy, information concerning microstructure fields. Of course, the price one must pay for such detail is often a case-by-case study rather than a general theory. Nevertheless, it should be recognized that, while general macrostructural - based theories may appear more elegant, such theories may not be practical for many applications due to the unreasonable burden placed upon the experimentalist to determine a multitude of constants and/or functions.

In this presentation, focus is placed upon several recent works by the author and co-workers concerning the construction of mixture theories with microstructure for laminated and fibrous composites. The discussion is limited to thermomechanical processes in composites with initial periodic microstructure. Particular emphasis is placed upon wave propagation and thermal diffusion.

The presentation is divided into five sections. The methodology associated with two theoretical construction techniques is given in Section 2 along with a brief survey of applications. These techniques are demonstrated via two examples in Sections 3 and 4. Finally, in an effort to illusidate the applicability and utility of the techniques, two applications to nonlinear problems are discussed in some detail in Section 5; these include comparisons between mixture theory, exact and/or experimental results.

2. METHODOLOGY AND SURVEY

A variety of construction procedures may be used to generate mixture theories with microstructure. Two such procedures are selected for discussion herein in view of their observed success in describing thermomechanical processes in composite materials.

The first procedure, which is illustrated in Section 3 by an elementary example, is the Differential-difference Method. This approach has been used to develop continuum models of wave propagation in linear elastic [4-9, 26] and linear viscoelastic [9-10] laminated composites, wave propagation in linear elastic fibrous composites [7-11], wave propagation and debonding in laminated composites [12], and thermal diffusion in laminated composites [13, 14]. The method consists of eight basic construction steps which may be summarized as follows: 1) the field quantities (all dependent variables) of each composite constituent are expanded in a suitable spatial series (this expansion, which amounts to discretization of the component domains, may range from a Taylor series for sufficiently simple geometries to topological multiplexes [15], e.g., finite elements, for complex geometries); 2) recurrence relations for the expansion coefficient-functions are obtained by use of the field equations and the series is telescoped; 3) application of interface continuity conditions lead to differential (in time) - finite difference (in space) equations; 4) an associated set of differential (in time) - functional difference equations is observed to contain, as a solution subset, solutions of the finite difference relations; 5) solutions of the functional equations are smooth fields which take on exact values at discrete spatial points; these smooth fields are now employed as dependent variables; 6) all spatial differences are expanded in a Taylor series - an operation which furnishes partial differential equations, i.e., a continuum model; 7) nondimensional variables and a small parameter representing the ratio of typical micro-to-macro dimensions is introduced and the operators are truncated according to an asymptotic procedure; 8) mixture equations result by algebraic manipulation.

The second procedure, illustrated in Section 4 by an elementary example, is the Regular Asymptotic Method. This approach has been

used to model nonlinear wave propagation in laminated [16] and fibrous [17-19] composites, and thermal diffusion in fibrous composites [20-21]. The method consists of six basic construction steps which may be summarized as follows: 1) based upon the particular composite and the process considered, an estimate of the order of magnitude of all field variables is made; 2) the field equations are re-scaled such that all dependent variables are O(1); in the process a small parameter is introduced which constitutes a measure of the ratio of micro-to-macro-dimensions of the problem; 3) the conservation equations are averaged to obtain a standard mixture form; 4) the scaled field variables are expanded in a regular asymptotic series; 5) the two lowest order systems (including interface conditions) are used to obtain expressions for the interaction terms and the constitutive relations; 6) the constants involved in 5) are obtained from the solution of a static micro boundary value problem defined over a unit cell; a variational principle - based finite element method is suggested to resolve this boundary value problem.

A judicious choice of a particular method depends upon the problem. The Differential-difference Method is best suited to linear problems and elementary geometries such as laminates. Here formally exact relations may be obtained in many cases. The Regular Asymptotic Method is, on the other hand, applicable to nonlinear problems and complex geometries. In this case one is usually content with the first few terms of the asymptotic series.

3. EXAMPLE 1: WAVE PROPAGATION

For the purpose of illustrating the Differential-difference Method, consider wave propagation in a periodic array of linearly elastic, homogeneous and isotropic laminae, perfectly bonded at all interfaces as illustrated in Fig. 1. Let $y \equiv x_2$ for notational convenience and assume a state of uniaxial motion in the y-direction; i.e., the case of one-dimensional longitudinal waves propagating normal to the laminae. Restricting attention to small isothermal deformations, the appropriate conservation and constitutive equations are

$$(\partial_y \sigma - \rho \partial_t^2 u)^{(\alpha,k)} = 0 \quad , \quad (\sigma - (\lambda+2\mu)\partial_y u)^{(\alpha,k)} = 0 \quad , \tag{1}$$

while the interface continuity conditions are

$$\{u,\sigma\}^{(1,k)}(h^{(1)},t) = \{u,\sigma\}^{(2,k)}(-h^{(2)},t) \quad ,$$

$$\{u,\sigma\}^{(1,k+1)}(-h^{(1)},t) = \{u,\sigma\}^{(2,k)}(h^{(2)},t) \quad . \tag{2}$$

In the above the superscripts (α,k) refer to the k^{th} layer of the α^{th} constituent, $\alpha = 1,2$; $k = 1,2,3\ldots$. The variable $y^{(\alpha,k)}$ is a local coordinate with origin at the midplane of the (α,k) layer; $\sigma \equiv \sigma_{22}$ and $u \equiv u_2$ are normal stress and displacement (subscripts on σ and u have been dropped for brevity). The quantities $\rho^{(\alpha)}$, $h^{(\alpha)}$, $\lambda^{(\alpha)}$, $\mu^{(\alpha)}$ are mass density, layer half thickness and Lame' constants for the α - constituent. In addition $\partial_y(\ ) \equiv \partial(\ )/\partial y$, $\partial_t(\ ) \equiv \partial(\ )/\partial t$.

Wave motion in the composite is completely specified by (1), (2)

together with initial conditions at t=0 and boundary data on y=0, H($H \leq \infty$). The objective of the subsequent work is to replace this set of equations (infinite if $H = \infty$) by a single set of partial differential equations which represent a continuum mixture theory.

3.1 Expansion, Recurrence Relations

Let us expand the stress and displacement about each lamina midplane as follows:

$$g(y^{(\alpha,k)}, t) = \sum_{n=0}^{\infty} g_{(n)}(t) y^{(\alpha,k)^n}/n! \quad . \tag{3}$$

Here g represents any of $\sigma^{(\alpha,k)}$, $u^{(\alpha,k)}$. Upon substituting (3) into (1) and equating powers of $y^{(\alpha,k)}$, one obtains the differential - recurrence relations

$$c^{(\alpha)^2}\{u,\sigma\}^{(\alpha,k)}_{(n+2)} = \partial_t^2\{u,\sigma\}^{(\alpha,k)}_{(n)} \quad , \quad \sigma^{(\alpha,k)}_{(n)} = \tilde{E}^{(\alpha)} u^{(\alpha,k)}_{(n+1)} \quad . \tag{4a}$$

Here

$$c^{(\alpha)^2} \equiv \tilde{E}^{(\alpha)}/\rho^{(\alpha)} \quad , \quad \tilde{E}^{(\alpha)} \equiv (\lambda+2\mu)^{(\alpha)} \quad , \tag{4b}$$

where $n = 0, 1, 2\ldots$; $k = 1, 2, 3, \ldots$; $\alpha = 1, 2$. With use of the recurrence relations (4a), the series (3) may be telescoped as follows

$$\{u,\sigma\}^{(\alpha,k)}(y^{(\alpha,k)}, t) = C^{(\alpha,k)}\{u,\sigma\}^{(\alpha,k)}_{(0)}(t) + y^{(\alpha,k)} S^{(\alpha,k)}\{\tilde{E}^{-1}\sigma, \rho\partial_t^2 u\}^{(\alpha,k)}_{(0)} \tag{5}$$

where $C^{(\alpha,k)}$, $S^{(\alpha,k)}$ are formal differential operators defined by

$$C^{(\alpha,k)} \equiv \cosh(c^{(\alpha)^{-1}} y^{(\alpha,k)} \partial_t) \quad ,$$

$$S^{(\alpha,k)} \equiv (c^{(\alpha)^{-1}} y^{(\alpha,k)} \partial_t)^{-1} \sinh(c^{(\alpha)^{-1}} y^{(\alpha,k)} \partial_t) \quad . \tag{6}$$

The functions $\sigma_{(0)}^{(\alpha,k)}(t)$, $u_{(0)}^{(\alpha,k)}(t)$ represent stress and displacement at the midplane of the (α,k) layer; these serve as dependent variables in the ensuing analysis.

3.2 Transition to a Continuum Theory

Substitution of the expansions (5) into the interface conditions (2) furnishes the following differential (in time) - finite difference (in space) equations with dependent variables defined at discrete points along the y-axis:

$$C^{(\alpha)}(u^{(\alpha,k+1)}_{(0)} + u^{(\alpha,k)}_{(0)}) - 2C^{(\beta)}u^{(\beta,k)}_{(0)} - h^{(\alpha)}\tilde{E}^{(\alpha)^{-1}} S^{(\alpha)}(\sigma^{(\alpha,k+1)}_{(0)} - \sigma^{(\alpha,k)}_{(0)}) = 0,$$

$$C^{(\alpha)}(\sigma^{(\alpha,k+1)}_{(0)} + \sigma^{(\alpha,k)}_{(0)}) - 2C^{(\beta)}\sigma^{(\beta,k)}_{(0)} - \rho^{(\alpha)} h^{(\alpha)} S^{(\alpha)} \partial_t^2 (u^{(\alpha,k+1)}_{(0)} - u^{(\alpha,k)}_{(0)}) = 0 \quad , \tag{7}$$

$\alpha, \beta = 1, 2;\ \alpha \neq \beta$.

If one now defines the fields

$$\{u,\sigma\}^{(\alpha)}(y,t) \equiv \{u,\sigma\}^{(\alpha,k)}(y,t) \quad \text{for} \quad y \in (Y^{(\alpha,k)} - h^{(\alpha)},\ Y^{(\alpha,k)} + h^{(\alpha)}) ,$$

$$\equiv \{0,0\} \quad \text{for} \quad y \in (Y^{(\beta,k)} - h^{(\beta)},\ Y^{(\beta,k)} + h^{(\beta)}) , \tag{8}$$

$\alpha, \beta = 1, 2;\ \alpha \neq \beta$; and if one notes that

$$\{u,\sigma\}^{(\alpha,k)}_{(0)}(t) = \{u,\sigma\}^{(\alpha)}(Y^{(\alpha,k)}, t) \quad , \qquad Y^{(2,k)} = Y^{(1,k)} + \Delta \ , \ \Delta \equiv h^{(1)} + h^{(2)} , \tag{9}$$

then (7) can be rewritten in the form

$$C^{(\alpha)}[u^{(\alpha)}(y+\Delta,t) + u^{(\alpha)}(y-\Delta,t)] - 2C^{(\beta)}u^{(\beta)}(y,t)$$

$$- h^{(\alpha)}\tilde{E}^{(\alpha)^{-1}} S^{(\alpha)}[\sigma^{(\alpha)}(y+\Delta,t) - \sigma^{(\alpha)}(y-\Delta,t)] = 0 \ , \tag{10a}$$

$$C^{(\alpha)}[\sigma^{(\alpha)}(y+\Delta,t) + \sigma^{(\alpha)}(y-\Delta,t)] - 2C^{(\beta)}\sigma^{(\beta)}(y,t)$$

$$- \rho^{(\alpha)} h^{(\alpha)} S^{(\alpha)} \partial_t^2 [u^{(\alpha)}(y+\Delta,t) - u^{(\alpha)}(y-\Delta,t)] = 0 \ , \tag{10b}$$

$\alpha, \beta = 1, 2;\ \alpha \neq \beta$. Equations (10a, b) were obtained by replacing the fields $\sigma^{(\beta)}(Y^{(\beta,k)}, t)$ and $u^{(\alpha)}(Y^{(\beta,k)} + \Delta, t)$, etc., by the smooth fields $\sigma^{(\beta)}(y, t)$, $u^{(\alpha)}(y+\Delta, t)$, etc., defined over the entire domain of the composite; here $Y^{(\alpha,k)}$ denotes the midplane of the (α,k) layer (see Fig. 1).

The functional difference equations (10a, b) contain, as a subset, the solutions of the finite difference equations (7). That is, the new fields satisfy (7) at $y = Y^{(\beta,k)}$. Therefore, the new dependent variables $u^{(\alpha)}$, $\sigma^{(\alpha)}$ are functions defined for all y which assume exact values at layer midplanes. Assuming the admissibility of such expansions, all sums and differences are now expanded about $\Delta = 0$ in a Taylor series; this leads to the partial differential equations

$$C^{(\alpha)}\bar{C}u^{(\alpha)} - h^{(\alpha)}\Delta\tilde{E}^{(\alpha)^{-1}} S^{(\alpha)}\bar{S}\partial_y \sigma^{(\alpha)} - C^{(\beta)}u^{(\beta)} = 0 \ ,$$

$$C^{(\alpha)}\bar{C}\sigma^{(\alpha)} - h^{(\alpha)}\Delta\rho^{(\alpha)} S^{(\alpha)}\bar{S}\partial_y \partial_t^2 u^{(\alpha)} - C^{(\beta)}\sigma^{(\beta)} = 0 \ , \tag{11}$$

$\alpha, \beta = 1, 2;\ \alpha \neq \beta$, where $\bar{C}$, $\bar{S}$ are formal differential operators of the form

$$\bar{C} \equiv \cosh(\Delta\partial_y) \ , \quad \bar{S} \equiv (\Delta\partial_y)^{-1} \sinh(\Delta\partial_y) \ . \tag{12}$$

Equations (11) constitute a continuum model of the composite. The dependent variables $u^{(\alpha)}$, $\sigma^{(\alpha)}$ of (11) can be used to reconstruct the microstructural fields through (5)(noting (8)).

3.3 Scaling

Let the typical "macrodimension" of the problem be ℓ and the typical "microdimension" be Δ. The quantity ℓ represent a dominant signal wavelength associated with wave motion. Introduce the non-

dimensional quantities

$$\zeta \equiv y/\ell \ , \quad \tau \equiv tc/\ell \ , \quad \epsilon \equiv \Delta/\ell \ , \quad \Sigma^{(\alpha)} \equiv \sigma^{(\alpha)}/\rho c^2 \ , \quad \eta^{(\alpha)} \equiv u^{(\alpha)}/\ell \tag{13}$$

where ρ, c denote appropriate mixture density and wave speed. Then (11) becomes

$$\begin{aligned} &C^{(\alpha)}\bar{S}\partial_\zeta \eta^{(\alpha)} - \mathcal{E}^{(\alpha)}\bar{C}S^{(\alpha)}\Sigma^{(\alpha)} - \mathcal{E}^{(\beta)}\mathcal{B}^{(\beta)}\Sigma^{(\beta)} = 0 \ , \\ &C^{(\alpha)}\bar{S}\partial_\zeta \Sigma^{(\alpha)} - \tilde{\rho}^{(\alpha)}\bar{C}\mathcal{B}^{(\alpha)}\partial_\tau^2 \eta^{(\alpha)} - \tilde{\rho}^{(\beta)}\mathcal{B}^{(\beta)}\partial_\tau^2 \eta^{(\beta)} = 0 \ , \end{aligned} \tag{14}$$

where

$$C^{(\alpha)} \equiv \cosh(\epsilon\gamma^{(\alpha)}\partial_\tau) \ , \quad S^{(\alpha)} \equiv (\epsilon\gamma^{(\alpha)}\partial_\tau)^{-1}\sinh(\epsilon\gamma^{(\alpha)}\partial_\tau) \ , \tag{15a}$$

$$\bar{C} \equiv \cosh(\epsilon\partial_\zeta) \ , \quad \bar{S} \equiv (\epsilon\partial_\zeta)^{-1}\sinh(\epsilon\partial_\zeta) \ , \quad \gamma^{(\alpha)} \equiv (c/c^{(\alpha)})n^{(\alpha)} \ , \tag{15b}$$

$$n^{(\alpha)} \equiv h^{(\alpha)}/\Delta \ , \quad \tilde{\rho}^{(\alpha)} \equiv n^{(\alpha)}\rho^{(\alpha)}/\rho \ , \quad \mathcal{E}^{(\alpha)} \equiv \rho c^2 n^{(\alpha)}/\tilde{E}^{(\alpha)} \ . \tag{15c}$$

The governing equations (14) are now scaled such that, if $y\in(0, \ell)$ and $\tau\in(0, \ell/c)$, then $\zeta\in(0, 1)$ and $\tau\in(0, 1)$; that is, the macrodimension is now $O(1)$ while the microdimension is $O(\epsilon)$. Thus, it is evident that all foregoing Taylor expansions about $\Delta=0$ are in fact expansions about $\epsilon = 0$; further, all operators are power series in $\epsilon^{(2n)}$, $n = 0, 1, 2\ldots$. Such expansions are not required to converge, but only be asymptotic as $\epsilon \to 0$ [4].

3.4 Binary Mixture Theories

With some algebraic manipulations, equations (14) may be rewritten in a form characteristic of binary - type mixture theories as follows:

$$\partial_\zeta\left[C^*C^{(\alpha)}\partial_\zeta\Sigma^{(\alpha)} - \tilde{\rho}^{(\alpha)}\mathcal{B}^{(\alpha)}\bar{S}\partial_\tau^2\eta^{(\alpha)}\right] = (-1)^{\alpha+1}\mathcal{R} \ , \tag{16a}$$

$$\partial_\zeta\left[C^*C^{(\alpha)}\partial_\zeta\eta^{(\alpha)} - \mathcal{E}^{(\alpha)}S^{(\alpha)}\bar{S}\Sigma^{(\alpha)}\right] = (-1)^{\alpha+1}\mathcal{P} \ , \tag{16b}$$

$\alpha = 1, 2$. Here

$$\epsilon^2\mathcal{P} \equiv C^{(2)}\Sigma^{(2)} - C^{(1)}\Sigma^{(1)} \ , \quad \epsilon^2\mathcal{R} \equiv C^{(2)}\eta^{(2)} - C^{(1)}\eta^{(1)} \ , \tag{16c,d}$$

$$C^* \equiv 1/2! + (\epsilon\partial_\zeta)^2/4! + (\epsilon\partial_\zeta)^4/6!\ldots \ . \tag{16e}$$

The bracket in (16a) suggests a momentum equation while that of (16b) has the character of a constitutive relation. The quantities $\mathcal{P}$ and $\mathcal{R}$ represent constituent interaction terms.

A mixture theory of order n is now defined as those equations obtained from (16a, b) by truncating the operators $C^{(\alpha)}C^*$ and $S^{(\alpha)}\bar{S}$, as well as the $C^{(\alpha)}$ in $\mathcal{P}$ and $\mathcal{R}$, after $O(\epsilon^{2n-2})$ terms. In particular, a mixture theory of order 1 is, under this definition, given by

$$\partial_\zeta(\partial_\zeta\Sigma/2 - \tilde{\rho}\partial_\tau^2\eta)^{(\alpha)} = (-1)^{\alpha+1}\rho^* \ , \ \partial_\zeta(\partial_\zeta\eta/2 - \rho\Sigma)^{(\alpha)} = (-1)^{\alpha+1}\mathcal{R}^* \quad (17a,b)$$

$$\epsilon^2\rho^* \equiv \Sigma^{(2)} - \Sigma^{(1)} \ , \ \epsilon^2\mathcal{R}^* \equiv \eta^{(2)} - \eta^{(1)} \ . \quad (18c,d)$$

Equations (17a) may be interpreted as mixture momentum relations and (17b) as mixture constitutive equations. The interaction terms in this formulation are proportional to displacement and stress differences, respectively.

The operator ∂_ζ preceding the left side of each equation (17a,b) can be eliminated by expanding the dependent variables in regular asymptotic series in ϵ. The result, upon retaining $O(\epsilon^2)$ terms only, is

$$\partial_\zeta\Sigma^{(\alpha p)} - \rho^{(\alpha p)}\partial_\tau^2\eta^{(\alpha)} = (-1)^{(\alpha)}\bar{\rho} \ , \ \bar{\rho} \equiv \mathcal{S}\partial_\tau^2(\eta^{(1)} - \eta^{(2)}) \quad (18)$$

where $\mathcal{S}$ is a constant which is a complicated function of composite geometry and material properties. The quantities $\Sigma^{(\alpha p)}$, $\rho^{(\alpha p)}$ here play the role of "partial" stresses and densities; their physical interpretation, however, is not obvious. Details concerning the derivation of (18), which shall be called a modified (first order) mixture theory, can be found in [4].

Let us now consider the limit as $\epsilon \to 0$ in (16). If it is assumed, that ℓ and c may be selected such that $\partial_\tau^n(\ ) = O(1)$, $\partial_\zeta^n(\ ) = O(1)$, $n = 1, 2\ldots$, where $(\ )$ represents $\eta^{(\alpha)}$ or $\Sigma^{(\alpha)}$, as $\epsilon \to 0$ (i.e., as the ratio of micro-to macro-dimensions vanishes), then (16) reduces in dimensional form to

$$[\partial_y^2 - (n^{(1)}\rho^{(1)} + n^{(2)}\rho^{(2)})(n^{(1)}\tilde{E}^{(1)^{-1}} + n^{(2)}\tilde{E}^{(2)^{-1}})\partial_t^2]\{u,\sigma\}^{(\alpha)} = 0. \quad (19)$$

Therefore, the theory is nondispersive as $\epsilon \to 0$, a result to be expected. Equation (19) implies that the appropriate mixture density ρ, modulus $\tilde{E}$, and wave speed c, are

$$\rho = n^{(1)}\rho^{(1)} + n^{(2)}\rho^{(2)} \ , \ \tilde{E}^{-1} = n^{(1)}\tilde{E}^{(1)^{-1}} + n^{(2)}\tilde{E}^{(2)^{-1}} \ , \ c^2 = \tilde{E}/\rho. \quad (20)$$

3.5 Phase Velocity Spectra

It is evident that the foregoing theory represents a long wavelength, low frequency approximation of composite wave motion. A natural question concerns the range of validity of this approximation. A convenient indication of the comparative accuracy of an approximate theory can be obtained by studying the phase velocity spectrum. Assuming steady-state sinusodal wave trains, equations (16), (17) or (18) become a set of homogeneous algebraic equations from which the relation between wave number k and phase velocity c_p is calculated. A typical comparison of exact, first order, and modified (first order) mixture phase velocity spectra is shown in Fig. 2 for a Polymethyl methacrylate (PMMA) - 304 stainless steel composite. The data shown represents the first mode of propagation down to the cutoff frequency associated with the first "stop band". The exact spectrum results from retaining all terms in the operators of (16) and is identical to that given by

Rytov [22]. Comparisons such as Fig. 2 indicate that reasonable accuracy may be expected from a theory of order 1 down to wavelengths equal to several microdimensions for problems where the energy is partitioned primarily in the first mode. This is quite a remarkable result for such an elementary theory. Additional details concerning the phase velocity spectrum as well as transient pulse calculations and an associated discussion concerning initial and boundary conditions can be found in [4-9].

4. EXAMPLE 2: HEAT CONDUCTION

For the purpose of illustrating the Regular Asymptotic Method, consider a linear thermal diffusion process in a periodic, two-dimensional array of unidirectional fibers of arbitrary cross section embedded in a matrix, as illustrated in Fig. 3a. Let a "cell" be associated with each fiber as depicted in Fig. 3b. Each such cell consists of regions $A^{(1)}$ and $A^{(2)}$ occupied by the fiber and matrix, respectively, with unit outer normals* $N_i^{(1)}$ and $N_i^{(2)}$. The interface between the two constituents shall be denoted by I, and the outer boundary of the cell by C. With respect to rectangular Cartesian coordinates x_1, x_2, x_3 as shown in Fig. 3a, let the composite occupy the domain $0 \le x_3 \le L$, $-\infty < x_2 < \infty$, $-\infty < x_1 < \infty$. Assume that the two constituents in each cell are homogeneous and isotropic with a perfect interface (no thermal resistance). Finally, let the initial conditions, and the boundary conditions on $x_3 = 0, L$ be such that the temperature field is <u>similar</u> in each cell. In view of the last premise it is sufficient to consider a typical cell with zero heat flux normal to the boundary C. Consequently the basic equations for the temperature fields $T^{(\alpha)}$ and heat flux vectors $Q_i^{(\alpha)}$, $\alpha = 1, 2$, are

$$(Q_{j,j} + d\dot{T})^{(\alpha)} = 0 \quad , \quad (Q_i + kT_{,i})^{(\alpha)} = 0 \quad \text{on } A^{(\alpha)} \; ; \tag{2 1a,b}$$

$$Q_\beta^{(2)} N_\beta^{(2)} = 0 \quad \text{on C;} \quad T^{(1)} = T^{(2)} \text{ and } (Q_\beta^{(1)} - Q_\beta^{(2)}) N_\beta^{(1)} = 0 \quad \text{on I.} \tag{2 1c,d}$$

Equation (2 1a) is the conservations of energy; the relation (2 1b) is the Fourier heat conduction law; equation (2 1c) is a symmetry condition; and (2 1d) represents the interface continuity of temperature and normal heat flux (note $N_3^{(\alpha)} = 0$). The superscript $\alpha = 1, 2$ refers to the fiber and the matrix, respectively. The quantities d, k denote heat capacity and thermal conductivity, respectively. The notations $(\;)_{,i} \equiv \partial(\;)/\partial x_i$ and $\dot{(\;)} \equiv \partial(\;)/\partial t$ have been introduced for convenience.

4.1 Scaling

Equations (2 1), together with initial conditions at t=0 and appropriate boundary data on $x_3 = 0, L$ specify a well posed problem involving <u>three</u> spatial variables x_i and time, t. The objective of the subsequent analysis is to derive a continuum mixture theory governing the macroscopic diffusion process which involves only <u>one</u> spatial dimension (x_3)

*Latin and Greek subscripts imply Cartesian tensors and the usual summation convention with ranges from 1 to 3 and 1 to 2 respectively.

and yet reflects, at least approximately, the effect of conduction on the microscale. To this end, let Λ and Δ be associated with typical "macroscopic" and "microscopic" observational dimensions, respectively. These lengths may be defined in terms of characteristic thermal diffusion times in the longitudinal and transverse directions according to

$$t_{(\Lambda)} \equiv d_{(m)}\Lambda^2/k_{(m)} \quad , \quad t_{(\Delta)} \equiv d_{(m)}\Delta^2/k_{(m)} \qquad (22)$$

where $d_{(m)}$, $k_{(m)}$ denote mixture heat capacity and thermal conductivity (to be defined later). In addition, it will be convenient to introduce a mixture heat flux $Q_{(m)}$ based upon a reference temperature T, and a parameter ϵ as follows:

$$Q_{(m)} \equiv k_{(m)}T/\Delta \quad , \quad \epsilon \equiv \Delta/\Lambda = (t_{(\Delta)}/t_{(\Lambda)})^{\frac{1}{2}} \quad . \qquad (23)$$

The quantity ϵ represents the ratio of micro-to-macro-dimensions of the composite.

With the aid of the foregoing definitions, the following non-dimensional variables are introduced

$$(\xi_3, \epsilon\xi_\beta) \equiv (x_3, x_\beta)/\Delta \quad , \quad \tau \equiv t/t_{(\Lambda)} \quad , \quad (\mathfrak{Q}_3, \epsilon\mathfrak{Q}_\beta)^{(\alpha)} \equiv (Q_3, Q_\beta)^{(\alpha)}/Q_{(m)} \quad , \qquad (23a)$$

$$\mathfrak{T}^{(\alpha)} \equiv T^{(\alpha)}/T \quad , \quad \mathfrak{d}^{(\alpha)} \equiv d^{(\alpha)}/d_{(m)} \quad , \quad \mathfrak{k}^{(\alpha)} \equiv k^{(\alpha)}/k_{(m)} \quad , \qquad (23b)$$

whence (21) become

$$(\mathfrak{Q}_{j,j} + \mathfrak{d}\dot{\mathfrak{T}})^{(\alpha)} = 0 \quad , \quad (\mathfrak{T}_{,3}, \epsilon^2\mathfrak{Q}_\beta)^{(\alpha)} + \mathfrak{k}^{(\alpha)}(\mathfrak{T}_{,3}\mathfrak{T}_{,\beta})^{(\alpha)} = 0 \quad \text{on } \mathfrak{C}^{(\alpha)}, \qquad (24a,b)$$

$$\mathfrak{Q}_\beta^{(2)}\nu_\beta^{(2)} = 0 \text{ on } \mathfrak{C} \; ; \; \mathfrak{T}^{(1)} = \mathfrak{T}^{(2)}, (\mathfrak{Q}_\beta^{(1)} - \mathfrak{Q}_\beta^{(2)})\nu_\beta^{(1)} = 0 \text{ on } \mathfrak{J} \; . \qquad (24c,d)$$

In (24) $\beta = 1, 2$ and $\mathfrak{C}^{(\alpha)}$, $\mathfrak{J}$, $\mathfrak{C}$ denote $A^{(\alpha)}$, I, C in nondimensional form; the vectors $\nu_\beta^{(\alpha)}$ are unit outer normals to the boundaries of $\mathfrak{C}^{(\alpha)}$; partial derivatives are now defined by $(\;)_{,i} \equiv \partial(\;)/\partial\xi_i$, $(\dot{\;}) \equiv \partial(\;)/\partial\tau$.

4.2 Mixture Equations

Binary mixture equations for this problem can be immediately obtained by averaging (24a) over $\mathfrak{C}^{(\alpha)}$ according to

$$\mathfrak{F}^{(\alpha a)}(\xi_3, \tau) = \mathfrak{C}^{(\alpha)^{-1}} \iint_{\mathfrak{C}^{(\alpha)}} \mathfrak{F}^{(\alpha)}(\xi_1, \xi_2, \xi_3, \tau)d\xi_1 d\xi_2 \qquad (25)$$

where $\mathfrak{F}^{(\alpha)}$ represents $\mathfrak{Q}^{(\alpha)}$ or $\mathfrak{T}^{(\alpha)}$. This yields, after a little algebraic manipulation

$$\mathfrak{Q}_{3,3}^{(\alpha p)} + \mathfrak{d}^{(\alpha p)}\dot{\mathfrak{T}}^{(\alpha p)} = (-1)^{\alpha+1}\mathfrak{p} \quad , \quad \mathfrak{p} \equiv \mathfrak{C}^{-1}\int_{\mathfrak{J}} \mathfrak{Q}_\beta^{(1)}\nu_\beta^{(1)}ds$$

$$= \mathfrak{C}^{-1}\int_{\mathfrak{J}} \mathfrak{Q}_\beta^{(2)}\nu_\beta^{(1)}ds \quad , \qquad (26a,b)$$

where

$$\mathfrak{Q}_3^{(\alpha p)} \equiv n^{(\alpha)} \mathfrak{Q}_3^{(\alpha a)} \ , \ \mathcal{d}^{(\alpha p)} = n^{(\alpha)} \mathcal{d}^{(\alpha)} \ , \ n^{(\alpha)} \equiv G^{(\alpha)} / (G^{(1)} + G^{(2)}) \ . \tag{27}$$

The quantities $\mathfrak{Q}_3^{(\alpha p)}$, $\mathcal{d}^{(\alpha p)}$, $n^{(\alpha)}$ represent partial heat fluxes, partial heat capacities, and volume fractions, respectively. The variable ρ is an interaction term reflecting heat transfer from the fiber to the matrix. At this stage the mixture equations (26) are exact. Approximations arise when one attempts to model the Fourier expressions for heat conduction, and the interaction term.

4.3 Asymptotic Expansions

A fundamental premise is now introduced: the ratio of the characteristic thermal diffusion times in the transverse and longitudinal (fiber axis) directions in small compared to unity, i.e.,

$$\epsilon^2 = t_{(\Delta)} / t_{(\Lambda)} = (\Delta / \Lambda)^2 << 1 \ . \tag{28}$$

Equation (28) is appropriate for many composites used for thermal protection. The premise (28) suggests the following regular asymptotic expansion for all dependent variables, denoted by $G^{(\alpha)}$:

$$G^{(\alpha)}(\xi_i, \tau; \epsilon) = \sum_{n=0}^{\infty} \epsilon^{2n} G_{(2n)}^{(\alpha)}(\xi_i, \tau) \ . \tag{29}$$

If (29) is substituted into the governing equations (24a, b) and the coefficients of similar ϵ-order are equated, one obtains a system of equations for each $n = 0, 1, 2 \ldots$. In what follows, a mixture theory is developed based on the lowest order system.

4.4 Interaction Term

The lowest order system corresponding to (24a, b) is

$$(\mathfrak{Q}_{j,j} + \mathcal{d}\dot{\mathfrak{T}})_{(0)}^{(\alpha)} = 0 \ , \ (\mathfrak{Q}_3 + \kappa \mathfrak{T}_{,3})_{(0)}^{(\alpha)} = 0 \ , \ (\mathfrak{T}_{,1} = \mathfrak{T}_{,2} = 0)_{(0)}^{(\alpha)} \ . \tag{30a,b,c}$$

Equations (30c) yield

$$\mathfrak{T}_{(0)}^{(\alpha)} = \mathfrak{T}_{(0)}^{(\alpha)}(\xi_3, \tau) \ , \tag{31}$$

whence, to lowest order accuracy, equations (25), (27) furnish

$$\mathfrak{Q}_3^{(\alpha p)} = - \kappa^{(\alpha p)} \mathfrak{T}_{,3}^{(\alpha p)}(\xi_3, \tau) \ . \tag{32}$$

In order to complete the mixture formulation, the functional dependence of the interaction term ρ on the averaged temperatures $\mathfrak{T}^{(\alpha a)}$ must be determined. For this purpose it is necessary to consider $\mathfrak{Q}_{\beta(0)}^{(\alpha)}$, $\mathfrak{T}_{(2)}^{(\alpha)}$ and to satisfy the continuity of temperature including $O(\epsilon^2)$ terms. To begin this task, one finds from (32) and (24b) that

$$\mathfrak{Q}_{\beta(0)}^{(\alpha)} = - \kappa^{(\alpha)} \mathfrak{T}_{(2),\beta}^{(\alpha)} \ . \tag{33}$$

Next, with use of (33) and (30b, c), equation (30a) becomes

$$(\mathcal{A}^{(\alpha)}\mathcal{T}^{(\alpha)}_{(2)})_{,\beta\beta} = \varphi^{(\alpha)}(\xi_3,\tau) \quad . \tag{34}$$

The functions $\varphi^{(\alpha)}$ can be related to ρ, defined by (26b), by integration of (34) over $\mathcal{C}^{(\alpha)}$, use of Gauss' Theorem, and the symmetry condition (24c); the result is:

$$n^{(\alpha)}\varphi^{(\alpha)} = (-1)^{\alpha}\rho \quad . \tag{35}$$

Thus, one obtains the following relations for $\mathcal{T}^{(\alpha)}_{(2)}$:

$$n^{(\alpha)}(\mathcal{A}^{(\alpha)}\mathcal{T}^{(\alpha)}_{(2),\beta})_{,\beta} = (-1)^{\alpha}\rho \text{ on } \mathcal{C}^{(\alpha)} (\alpha,\beta = 1,2) \quad . \tag{36}$$

The appropriate boundary conditions are, from (24c, d),

$$\mathcal{T}^{(2)}_{(2),\beta}\nu^{(2)}_{\beta} = 0 \text{ on } \mathcal{C}\,, \quad (\mathcal{A}^{(1)}\mathcal{T}^{(1)}_{(2),\beta} - \mathcal{A}^{(2)}\mathcal{T}^{(2)}_{(2),\beta})\nu_{\beta} = 0\,,$$

$$\mathcal{T}^{(2)}_{(2)} - \mathcal{T}^{(1)}_{(2)} = (\mathcal{T}^{(1)}_{(0)} - \mathcal{T}^{(2)}_{(0)})/\epsilon^2 \text{ on } \mathcal{J} \quad . \tag{37}$$

Equations (36), (37) constitute a "micro" boundary value problem in the ξ_1, ξ_2 - plane; the solution is unique within a function $\mathcal{H}(\xi_3,\tau)$. Once $\mathcal{T}^{(\alpha)}_{(2)}$ are known, one can write

$$\mathcal{T}^{(\alpha)} = [\mathcal{T}^{(\alpha)}_{(0)} + \epsilon^2\mathcal{H} \equiv \tilde{\mathcal{T}}^{(\alpha)}_{(0)}(\xi_3,\tau)] + \epsilon^2\rho\mathcal{T}^{*(\alpha)}(\xi_1,\xi_2) + O(\epsilon^4) \tag{38}$$

where

$$\rho\mathcal{T}^{*(1)} \equiv \mathcal{T}^{(1)}_{(2)} \quad , \quad \rho\mathcal{T}^{*(2)} \equiv \mathcal{T}^{(2)}_{(2)} + (\tilde{\mathcal{T}}^{(2)}_{(0)} - \tilde{\mathcal{T}}^{(1)}_{(0)})/\epsilon^2 \quad . \tag{39}$$

Upon averaging (39), one obtains

$$\mathcal{T}^{(\alpha a)}(\xi_3,\tau) = \tilde{\mathcal{T}}^{(1)}_{(0)}(\xi_3,\tau) + \epsilon^2\rho\mathcal{T}^{*(\alpha a)} \quad . \tag{40}$$

Hence, the interaction term can be written

$$\rho = a(\mathcal{T}^{(1a)} - \mathcal{T}^{(2a)})/\epsilon^2 \quad , \quad a \equiv (\mathcal{T}^{*(1a)} - \mathcal{T}^{*(2a)})^{-1} \quad . \tag{41a, b}$$

Equations (41a), (32), (26a) close the mixture theory. The primary result is expression (41b), which can be used to determine the interaction coefficient, a, for <u>arbitrary</u> fiber and/or cell geometry via the solution of a <u>time independent</u> problem defined over the unit cell. In terms of $\mathcal{T}^{*(\alpha)}$, this problem takes the form:

$$n^{(\alpha)}(\mathcal{A}^{(\alpha)}\mathcal{T}^{*(\alpha)}_{,\beta})_{,\beta} = (-1)^{\alpha} \text{ on } \mathcal{C}^{(\alpha)} \quad ; \tag{42}$$

$$\mathcal{T}^{*(2)}_{,\beta}\nu^{(2)}_{\beta} = 0 \text{ on } \mathcal{C}\,; \quad \mathcal{T}^{*(1)} = \mathcal{T}^{*(2)}\,, \quad (\mathcal{A}^{(1)}\mathcal{T}^{*(1)}_{,\beta} - \mathcal{A}^{(2)}\mathcal{T}^{*(2)}_{,\beta})\nu_{\beta} = 0 \text{ on } \mathcal{J}, \tag{43}$$

$$\mathcal{T}^{*(1)} = 0 \text{ at point } 0 \in \mathcal{C}^{(1)} \quad . \tag{44}$$

In general it is difficult to obtain an analytical solution to the above micro boundary value problem. As an alternative, a finite element procedure has been proposed [21] which may be utilized for

arbitrary two-dimensional cell geometry. This procedure is based upon a modified Reissner-type variational principle, the corresponding functional of which is defined by

$$\Pi = \sum_{\alpha=1}^{2} \int_{\Omega^{(\alpha)}} \left[\tfrac{1}{2} A_{\beta\beta}^{(\alpha)} \mathfrak{I}_{,\beta}^{*(\alpha)} \mathfrak{I}_{,\beta}^{*(\alpha)} + \frac{(-1)^{(\alpha)}}{n^{(\alpha)}} \pi^{*(\alpha)} \right] d\Omega + \oint_{\mathcal{S}} \mathfrak{D}^{*} (\mathfrak{I}^{*(1)} - \mathfrak{I}^{*(2)}) ds \qquad (45)$$

which is defined in terms of $\mathfrak{I}^{*(\alpha)}$ on $\Omega^{(\alpha)}$ and $\mathfrak{D}^{*}$ on $\mathcal{S}$. The equations for $\mathfrak{I}^{*(\alpha)}$ follow from the requirement Π be stationary with respect to arbitrary variations of $\pi^{*(\alpha)}$ and $\mathfrak{D}^{*}$; here $\mathfrak{D}^{*}$ is a Lagrange multiplier which physically represents the heat flux normal to the boundary $\mathcal{S}$.

4.5 Numerical Results

The finite element procedure has been used for the solution of the temperature microstructure problem and the interaction coefficient for a variety of geometries and combination of material properties. Details of such calculations can be found in [21]. Here several results of particular interest are noted; properties used are listed in Table 3.

A frequent fibrous composite geometry is a hexagonal array of circular cylindrical fibers. In practice it is common to approximate the cell geometry of this case by concentric circular cylinders [20]. Numerical results, based on the theory presented herein, related to the accuracy of this approximation are shown in Fig. 4, where the interaction coefficient has been calculated as a function of fiber volume fraction and thermal conductivity. From the data, the conclusion can be drawn that for a practical range of fiber volume fractions, the concentric cylinder approximation can be used without any significant loss of accuracy.

For calculation of the interaction coefficient, the concentric circular cylinders approximation based on equal fiber volume fraction can also be used for composites containing square fibers arranged in a square array. This is borne out by the results shown in Fig. 5.

The fields $\mathfrak{I}^{*(\alpha)}(\xi_1, \xi_2)$ needed to calculate the interaction term can also be used for the calculation of the temperature distribution in a unit cell. From (38)-(40) one has

$$\mathfrak{I}^{(\alpha)}(\xi_i, \tau) = \mathfrak{I}^{(\alpha a)} + a[\mathfrak{I}^{(1a)} - \mathfrak{I}^{(2a)}][\mathfrak{I}^{*(\alpha)} - \mathfrak{I}^{*(\alpha a)}] \ . \qquad (46)$$

In the right side of (46) the only quantity dependent upon inplane coordinates ξ_1 and ξ_2 is $\mathfrak{I}^{*(\alpha)}$. It follows, therefore, that curves of equal $\mathfrak{I}^{*(\alpha)}$ are also isothermal lines within the framework of the mixture theory. For this reason, and to illustrate the type of temperature microstructure that can be obtained from the mixture theory, contours of equal $\mathfrak{I}^{*(\alpha)}$, suitably normalized, are given in Fig. 6 for square fibers in a similar array.

Finally, an indication of the accuracy of the proposed mixture model and the construction procedure can be obtained by comparison of mixture-predicted response with 2D or 3D computer code calculations. This has been accomplished in [20] for the case of concentric circular

cylinders where two spatial dimensions and time are involved. Calculations were conducted to determine the evolution of the temperature field in a quescent half-space $x_3 \geq 0$ subject to the boundary condition

$$T(0, r, t) = \begin{cases} 1, & 0 \leq t \leq t_o \\ 0, & t > t_o \end{cases} . \qquad (47)$$

Both the mixture equations and the full 2D problem were solved by finite difference schemes [20]; the latter was used as the correlating norm for estimating the accuracy of the mixture theory solutions. Fig. 7 illustrates typical average temperature profiles in the two constituents after a short time following the termination of the temperature pulse. The ability of the mixture theory to predict the temperature microstructure is illustrated in Fig. 8; the radial distribution of temperature obtained from the mixture theory is almost identical to the exact solution.

4.6 Remarks

The significant feature of the above mixture theory, and of similar theories proposed for wave propagation [16-19], is that it converts what is essentially a three-dimensional problem to a problem involving a single spatial variable, without losing the essential details of local field distributions. The reduction in the number of dependent variables leads, of course, to a substantial increase in numerical efficiency.

5. SELECTED APPLICATIONS

Two applications involving nonlinear wave propagation are briefly reviewed in this section in an effort to demonstrate the utility of mixture theories with microstructure. The first involves delamination of laminated composites. The second concerns finite amplitude elastic-plastic wave propagation in fibrous composites.

5.1 Wave Propagation and Debonding in Laminated Composites

A "first order" mixture theory with microstructure has been developed in [12] for longitudinal wave propagation and debonding in a laminated, binary composite with periodic microstructure. The case considered concerns small isothermal deformations, linear elastic constituents, and a Mohr-Coulomb interface failure and slip model. In view of the last item the problem is nonlinear. With respect to Fig. 1, a condition of plane strain was assumed in the x_3-direction and wave motion yielding symmetric velocity v_1 and anti-symmetric velocity v_2 distributions with respect to the x_2-coordinate within each lamina. Theoretical construction was based on the Differential-difference Method. In dimensional form, and with reference to Fig. 1, the relevant equations are

$$\sigma_{11,1}^{(\alpha p)} - \rho^{(\alpha p)}\ddot{u}_1 = (-1)^{\alpha+1}P \ , \quad \sigma_{11}^{(\alpha p)} = \sum_{\gamma=1}^{2} c^{(\alpha\gamma)} u_{1,1}^{(\gamma a)} \ , \tag{48a,b}$$

$$\dot{P} = K(\dot{u}_1^{(1a)} - \dot{u}_1^{(2a)}) \quad \text{if} \quad P < |P_{cr}| \ ,$$

$$P = \left(\frac{A - B\sigma_{22}^{*}}{h^{(1)}+h^{(2)}}\right) \mathrm{sgn}(\dot{u}_1^{(1a)} - \dot{u}_1^{(2a)}) \quad \text{if} \quad P = |P_{cr}| \ . \tag{48c}$$

Equations (48a) are mixture momentum equations while (48b) represent mixture constitutive relations. The quantity P denotes a momentum interaction term. The variables $\sigma_{11}^{(\alpha p)}$, $\rho^{(\alpha p)}$ denote partial quantities and are defined by $(\ )^{(\alpha p)} \equiv n^{(\alpha)}(\ )^{(\alpha a)}$ where $(\ )^{(\alpha a)}$ is an averaged variable and $n^{(\alpha)} \equiv h^{(\alpha)}/(h^{(1)} + h^{(2)})$. The quantity $|P_{cr}|$ is related to the interface shear stress σ_{12}^{*} and normal stress σ_{22}^{*} by

$$(h^{(1)}+h^{(2)})|P_{cr}| \equiv |\sigma_{12}^{*}|_{cr} = A - B\sigma_{22}^{*} \quad (\sigma_{22} \le 0) \ ,$$

$$\sigma_{22}^{*} = (n^{(1)}\lambda^{(1)}E^{(2)}u_{1,1}^{(1a)} + n^{(2)}\lambda^{(2)}E^{(1)}u_{1,1}^{(2a)})/(n^{(1)}E^{(2)} + n^{(2)}E^{(1)}) \ . \tag{49}$$

The constants A, B represent interface cohesion and frictional coefficients, respectively. The constants $c^{(\alpha\beta)}$, K are given in terms of the composite properties and geometry by

$$K \equiv 3\mu^{(1)}\mu^{(2)}/(h^{(1)}+h^{(2)})^2(n^{(1)}\mu^{(1)} + n^{(2)}\mu^{(2)}) \ , \quad c^{(\alpha\alpha)} \equiv n^{(\alpha)}E^{(\alpha)} - \frac{\lambda^{(\alpha)2}}{E} \ ,$$

$$c^{(\alpha\beta)} \equiv \frac{\lambda^{(\alpha)}\lambda^{(\beta)}}{E} \ , \quad E \equiv \frac{E^{(1)}}{n^{(1)}} + \frac{E^{(2)}}{n^{(2)}} \ , \quad E^{(\alpha)} \equiv (\lambda+2\mu)^{(\alpha)}, \quad (\alpha,\beta=1,2;\ \alpha\neq\beta), \tag{50}$$

where λ, μ are Lame' constants.

Considerable insight into the modeling capability of the above mixture theory can be gained by comparison of theoretical calculations with the experimental impact data on delaminated plates reported in [23]. The composites in this study consisted of alternating layers of Polymethyl methacrylate (PMMA, Rohm and Haas type A) 0.762 mm thick, and 6061-T6 aluminum 0.792 mm thick. The laminae of the composite were oriented perpendicular to the impact plane, and struck by a projectile from a 10cm bore light gas gun. An aluminum buffer plate 1.0cm thick was placed at the rear of the composite to improve planarity of the transmitted wave front. A transparent Dynasil 100 window followed the buffer, and a thin mirror was vapor deposited at the buffer window interface. The motion of the mirror was monitored to within $\pm 1.5 \times 10^{-5}$mm by means of a displacement interferometer. The experimental configuration reproduced from [23] is depicted in Fig. 9. The shot matrix is summarized in Table 1.

The mixture theory, consisting of (48) was coded in finite difference form and solved numerically. Material properties for the

composite laminates, flyer plate material, buffer and window materials are listed in Table 1. Input to the computer code required only the material properties of all constituents, goemetries of the test configuration, and flyer impact velocity. Numerical values for A and B were determined by a parametric study on the results of experimental shot number 2. They were found to be $A = 0.01 \times 10^9$ dynes/cm^2 and $B = 0.50$. All other correlations were performed using these values. Typical results are depicted in Figs. 10-12. As can be seen, agreement is generally excellent. Both theoretical and experimental results clearly exhibit the effects of bond breakage and delamination. This is manifested by the appearance of a precursor at the front of the wave profile and by greatly reduced oscillations behind the wave front when compared with both theoretical and experimental results for perfectly bonded waveguides (e.g., see [12]).

5.2 Nonlinear Wave Propagation in Fibrous Composites

A binary, first-order mixture theory with microstructure has been developed in [17], using the Regular Asymptotic Method and the concentric cylinders approximation, for nonlinear waveguide-type propagation parallel to the fibers of a unidirectionally reinforced fibrous composite with initial periodic hexagonal array, Fig. 13. The resulting model incorporates the effects of thermodynamics, finite deformation, and elastic-plastic constituents. The constitutive relations for this analysis consist of a Mie-Grüneisen equation of state which relates mean pressure, density, and internal energy, and a von Mises-type yield cirteria and associated (J_2) flow rule which govern the stress derivators. Under the assumption of an adiabatic process and isotropic, homogeneous constituents, the following mixture theory was obtained for composites with perfect bonds

(a) Continuity:

$$\sum_{\alpha=1}^{2} n^{(\alpha)} f^{(\alpha a)} = 0 \quad , \quad f^{(\alpha a)} \equiv -\left[\left(\rho^{(\alpha a)} v_3^{(\alpha a)}\right)_{,3} + \dot{\rho}^{(\alpha a)}\right] / \rho^{(\alpha a)} \quad . \tag{51}$$

(b) Momentum:

$$\left[n^{(\alpha)}\left(-p+S_{33}\right)^{(\alpha a)}\right]_{,3} - n^{(\alpha)} \rho^{(\alpha a)} D_t^{(\alpha a)} v_3^{(\alpha a)} = (-1)^{\alpha+1} P \quad , \tag{51a}$$

where

$$\sum_{\alpha=1}^{2} n^{(\alpha)} B^{(\alpha)} \mathfrak{L}^{(\alpha a)}\left[\frac{P+(-1)^{\alpha}\left(-p+S_{33}\right)^{(\alpha a)} n_{,3}^{(\alpha)}}{n^{(\alpha)}}\right]$$

$$- (-1)^{\alpha} n^{(\alpha)} B^{(\alpha)} f_{,3}^{(\alpha a)} = \frac{8\left(v_3^{(1a)} - v_3^{(2a)}\right)}{r_2^2} \quad , \tag{51b}$$

$$\mathfrak{L}^{(\alpha a)}(\ ) \equiv \mu^{(\alpha)^{-1}} D_t^{(\alpha a)}(\ ) + 2\Lambda^{(\alpha a)}(\ ) \quad , \quad D_t^{(\alpha a)}(\ ) \equiv (\dot{}) + v_3^{(\alpha a)}(\ )_{,3} \quad , \tag{51c}$$

$$B^{(1)} \equiv 1 \ , \ B^{(2)} \equiv - (2/n^{(2)})^2 (\frac{3}{2} - 2n^{(1)} + \frac{1}{2} n^{(1)^2} + \ln n^{(1)}) \ . \tag{51d}$$

(c) Energy:

$$\sum_{\alpha=1}^{2} n^{(\alpha)} [\rho^{(\alpha a)} D_t^{(\alpha a)} e^{(\alpha a)} - (-p+S_{33})^{(\alpha a)} v_{3,3}^{(\alpha a)}] = (-1)^{\alpha+1} R \ , \tag{52a}$$

$$R = (-p+S_{rr})^{(1a)} n^{(1)} f^{(1a)} \ . \tag{52b}$$

(d) Caloric equation of state (Mie-Grüneisen):

$$p^{(\alpha a)} = g(\rho^{(\alpha a)}) + \Gamma(\rho^{(\alpha a)}) \rho^{(\alpha a)} e^{(\alpha a)} \ . \tag{53}$$

(e) Stress derivator constitutive relations:

$$\mathfrak{L}^{(\alpha a)} S_{33}^{(\alpha a)} = \frac{4}{3} (v_{3,3}^{(\alpha a)} - \frac{1}{2} f^{(\alpha a)}) \ , \ S_{\theta\theta}^{(1a)} = S_{rr}^{(1a)} = -\frac{1}{2} S_{33}^{(1a)} \ , \tag{54a}$$

$$\mathfrak{L}^{(2a)} S_{rr}^{(2a)} = - \frac{2}{3} [v_{3,3}^{(\alpha a)} - \frac{1}{2} f^{(\alpha a)} (1 + \frac{3}{n^{(2)}} \ln \frac{1}{n^{(1)}})] \ , \tag{54b}$$

$$S_{\theta\theta}^{(2a)} = - (S_{rr}^{(2a)} + S_{33}^{(2a)}) \ , \tag{54c}$$

where

$$\Lambda^{(\alpha a)} = 0 \ \text{ if } \ J_2^{(\alpha a)} < \frac{1}{3} Y^{(\alpha)^2} \ \text{ or } \ D_t^{(\alpha a)} J_2^{(\alpha a)} < 0 \ ,$$

$$= \frac{3}{2} Y^{(\alpha)^2} [S_{33}^{(\alpha a)} v_{3,3}^{(\alpha a)} + S_{rr}^{(\alpha a)} f^{(\alpha a)}] \ \text{ if } \ D_t^{(\alpha a)} J_2^{(\alpha a)} \geq 0$$

$$\text{and } \ J_2^{(\alpha a)} = \frac{Y^{(\alpha)^2}}{3} \ . \tag{54d}$$

(f) Interface stress match:

$$(-p+S_{rr})^{(1a)}(x_3, t) = (-p+S_{rr})^{(2a)}(x_3, t) \ . \tag{55}$$

(g) Volume fractions:

$$D_t^{(1a)} n^{(1)} = n^{(1)} f^{(1a)} \ , \ n^{(1)} + n^{(2)} = 1 \ . \tag{56}$$

(h) Definition of averages:

$$(\ )^{(1a)} \equiv \frac{1}{\pi r^{(1)^2}} \int_0^{r^{(1)}} 2\pi r (\ )^{(1)} dr \ , \tag{57a}$$

$$( )^{(2a)} \equiv \frac{1}{\pi(r^{(2)^2} - r^{(1)^2})} \int_{r^{(1)}}^{r^{(2)}} 2\pi r( )^{(2)} dr \ . \qquad (57b)$$

The dependent variables above number 14. These are $n^{(\alpha)}, \rho^{(\alpha a)}$, $v_3^{(\alpha a)}$, $p^{(\alpha a)}$, $S_{33}^{(\alpha a)}$ and $e^{(\alpha a)} (\alpha = 1, 2)$. The foregoing represent volume fraction, density, velocity component in the x_3-direction, stress deviator component in the x_3-direction, and internal energy, respectively. Equations (51)-(56) constitute 14 independent relations for the above unknowns. The independent variables, which were originally r, θ, x_3, t (see Fig. 13), are now x_3, t only. All equations are written in an Eulerian description. It should be noted that $\alpha = 1$ refers to the fiber while $\alpha = 2$ denotes the matrix.

In an effort to test the validity of the first-order mixture theory, a comparison was made between calculations performed using the quasi-one-dimensional mixture equations, and a formal two-dimensional solution of the concentric cylinders problem. The mixture solutions were obtained by writing (50-56) in finite difference form and solving simultaneously for the 14 dependent variables. The necessary numerical analysis and the resulting code is described in [24]. The two-dimensional solutions were generated using a well-known Lagrangian finite difference computer code called CRAM [25]. A typical cell of a quartz-phenolic composite occupying the half-space $x_3 < 0$ was selected for study. For computation in the range $0 \leq p \leq 30$ K bar a Mie-Grüneisen relation of the form

$$p^{(\alpha a)} = \sum_{i=1}^{3} H_i^{(\alpha)} \eta^{(\alpha)} + G^{(\alpha)} \rho^{(\alpha a)} e^{(\alpha a)} \ , \quad \eta^{(\alpha)} \equiv \rho^{(\alpha a)} / \rho_{(I)}^{(\alpha)} - 1 \ ; \qquad (58)$$

was used, where $\rho_{(I)}^{(\alpha)}$ denotes the initial density of material α, and $H_i^{(\alpha)}$, $G^{(\alpha)}$ are material constants. The constituent material properties employed in all calculations are given in Table 2. Quiescent initial conditions were assumed. Boundary conditions consisted of a particle velocity of 0.5cm/μ sec of 1.0-μ sec duration applied uniformly to both constituents at $x_3 = 0$.

A comparison of mixture theory and two-dimensional finite difference code predictions of averaged constituent particle velocity as a function of time is illustrated in Figs. 14, 15. The two-dimensional code prediction, which resolves the particle velocity distributions in the radial direction, where averaged according to (57) in order to provide direct comparisons with the mixture theory. Results are shown for a propagation (x_3-direction) distance of 0.5cm. Agreement between the finite difference and mixture theory calculations is judged to be excellent. Finally, it is noted that on the same computer (aUNIVAC 1108), the CRAM calculation required roughly 500 times the computer time needed for the equivalent mixture calculation.

REFERENCES

1. BOWEN, R. M., Theory of Mixtures, in Continuum Physics, Vol. III, Academic Press, New York, 1976, 1-129
2. ATKIN, R. J. and CRAINE, R. E., Continuum Theories of Mixtures: Basic Theory and Historical Development, Q. Jl. Mech. Appl. Math., 29, 1976, 209-244.
3. ATKIN, R. J. and CRAINE, R. E., Continuum Theory of Mixtures: Applications, J. Inst. Maths. Applics. 17, 1976, 153-207.
4. HEGEMIER, G. A. and NAYFEH, A. H., A Continuum Theory for Wave Propagation in Laminated Composites-Case 1: Propagation Normal to the Laminates, J. Appl. Mech., 40, 1973, 503-510.
5. HEGEMIER, G. A. and BACHE, T. C., A Continuum Theory for Wave Propagation in Laminated Composites-Case 2: Propagation Parallel to the Laminates, J. Elast., 3, 1973, 125-140.
6. HEGEMIER, G. A. and BACHE, T. C., A General Continuum Theory with Microstructure for Wave Propagation in Elastic Laminated Composites, J. Appl. Mech., 41, 1974, 101-105.
7. HEGEMIER, G. A., GURTMAN, G. A., NAYFEH, A. H., A Continuum Mixture Theory of Wave Propagation in Laminated and Fiber Reinforced Composites, Int. J. Solids Structures, 9, 1973, 1973, 395-414.
8. NAYFEH, A. H., Time Harmonic Waves Propagation Normal to the Layers of a Multilayered Periodic Media, J. Appl. Mech., 41, 1974, 92-96.
9. BACHE, T. C., A Continuum Theory with Microstructure for Wave Propagation in Composite Materials, Ph. D Dissertation, University of California, San Diego, 1973.
10. HEGEMIER, G. A., BACHE, T. C., A General Continuum Theory for Viscoelastic Laminated Composites, Air Force Office of Scientific Research Technical Report AFOSR 74-0135, 1974.
11. WEITSMAN, Y., A Mixture Theory for Longitudinal Waves in Materials Reinforced by Rectangular Fiber Arrays, Acta Mechanica, 1976.
12. GURTMAN, G. A., and HEGEMIER, G. A., A Mixture Theory for Wave Guide-Type Propagation and Debonding in Laminated Composites, Int. J. Solids Structures, 11, 1975, 973-984.
13. MAEWAL, A., BACHE, T. C., and HEGEMIER, G. A., A Continuum Model for Diffusion in Laminated Composite Media, J. Heat Transfer, 98, 1976, 133-138.
14. NAYFEH, A. H., A Continuum Mixture Theory of Heat Conduction in Laminated Composites, J. Appl. Mech., 42, 1975, 399-404.
15. ODEN, J. T., Finite Elements of Nonlinear Continua, McGraw-Hill 1972.
16. HEGEMIER, G. A., Finite Amplitude Elastic-Plastic Wave Propagation in Laminated Composites, J. Appl. Phys., 45, 4248-4253.
17. HEGEMIER, G. A. and GURTMAN, G. A., Finite-Amplitude Elastic-Plastic Wave Propagation in Fiber-Reinforced Composites, J. Appl. Phys., 45, 1974, 4254-4261.

18. MURAKAMI, H., Maewal, A., and HEGEMIER, G.A., Mixture Theory for Longitudinal Wave Propagation in Unidirectional Composites with Cylindrical Fibers of Arbitrary Cross Section, I: Formulation, to be submitted for publication.
19. MURAKAMI, H., MAEWAL, A., and HEGEMIER, G.A., Mixture Theory for Longitudinal Wave Propagation in Unidirectional Composites with Cylindrical Fibers of Arbitrary Cross Section, II: Numerical, results to be submitted for publication.
20. MAEWAL, A., GURTMAN, G.A., and HEGEMIER, G.A., A Mixture Theory for Quasi-One-Dimensional Diffusion in Fiber-Reinforced Composites, to appear in J. Heat Transfer.
21. MURAKAMI, H., HEGEMIER, G.A., and MAEWAL, A., A Mixture Theory for Thermal Diffusion in Unidirectional Composites with Cylindrical Fibers of Arbitrary Cross Section, to be submitted for publication.
22. RYTOV, S.M., Acoustical Properties of a Thinly Laminated Medium, Soviet Phys. Acoustics, 2, 1965, 65-77.
23. DRUMHELLER, D.S., and LUNDERGAN, C.D., On the Behavior of Stress Waves in Composite Materials-II: Theoretical and Experimental Studies on the Effects of Constituent Debonding, Int. J. Solids and Structures, 11, 1975.
24. GURTMAN, G.A., NAYFEH, A.H., HEGEMIER, G.A., SIMS, E.W., BROWNELL, D.H., Systems, Science and Software Co. Report No., AFWL-TR-73-41, 1973 (unpublished).
25. SEDGWICK, R.T., WOLFGANG, D.A., General Electric Missiles and Space Division Report No. 69Sd1002, 1969 (unpublished).
26. NAYFEH, A.H., and GURTMAN, G.A., A Continuum Approach to the Propagation of Shear Waves in Laminated Wave Guides, J. Appl. Mech., 41, 1974, 106-110.

ACKNOWLEDGEMENTS

Research was sponsored by the Air Force Office of Scientific Research under Contract F49620-76-C-0024.

LIST OF FIGURES

LIST OF TABLES

Table 1. The Experimental Configurations.*

Experiment No.	Composite thickness (cm)	Projectile		
		Material	Velocity (cm/μsec)	Thickness (cm)
1†	0.820	Aluminum	0.001355	1.634
2	0.776	Aluminum	0.001420	1.631
3	0.806	Aluminum	0.001144	1.571
4	0.803	PMMA	0.002118	0.691
5	0.805	PMMA	0.003078	0.694
6	0.812	Tungsten Carbide	0.001289	0.975
7	0.810	Aluminum	0.001330	0.656
8	0.809	Aluminum	0.001066	0.164

* In all experiments the buffer plate was 1 cm thick. The bond thicknesses were all less than 0.0002 cm thick.

† Experiment 1 exhibited excessive flyer tilt and Drumheller and Lundergan considered the data useless.

Table 2

Material Properties used in TINC and CRAM Calculations

	Material 1	Material 2
Initial Density $\rho_I^{(\alpha)}$ (g/cc)	1.85	1.29
Shear Modulus, $\mu^{(\alpha)}$ (dynes/cm^2)	106.0 (10^9)	30.3 (10^9)
Bulk Modulus, $H_1^{(\alpha)}$ (dynes/cm^2)	397.6 (10^9)	96.0 (10^9)
$H_2^{(\alpha)}$ (dynes/cm^2)	38.0 (10^{11})	0
$H_3^{(\alpha)}$ (dynes/cm^2)	275.0 (10^{11})	11.3 (10^{11})
Mie-Grüneisen Ratio, $G^{(\alpha)}$	.32	.52
Yield Stress in Simple Tension $Y^{(\alpha)}$ (dynes/cm^2)	2.75 (10^9)	1.33 (10^9)

Radial Fiber Radius, r_1 (cm)	0.08
Outer Cylinder Radius r_2 (cm)	0.20

TABLE 3

MATERIAL PROPERTIES USED FOR COMPUTATIONS

Thermal Conductivity Ratio	$\frac{\bar{k}^{(1)}}{\bar{k}^{(2)}} = 50$
Specific Heat Ratio	$\frac{\bar{\mu}^{(1)}}{\bar{\mu}^{(2)}} = 0.5$
Volume Fractions	$n_1 = .2$ (Fiber), $n_2 = .8$ (Matrix)

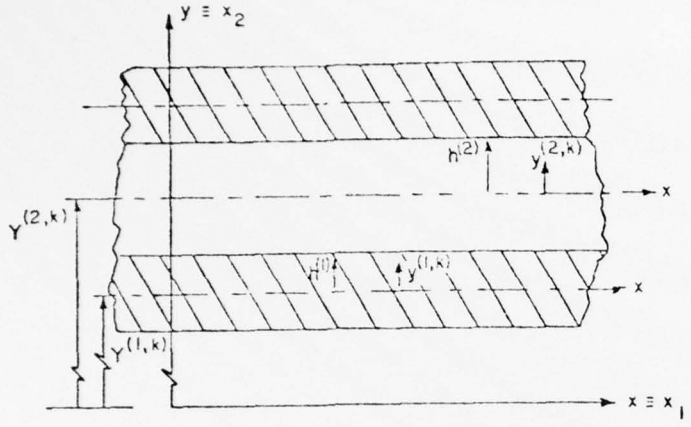

Fig. 1

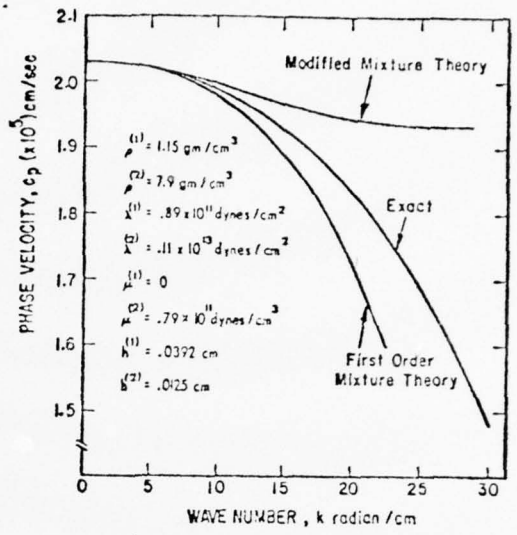

Fig. 2

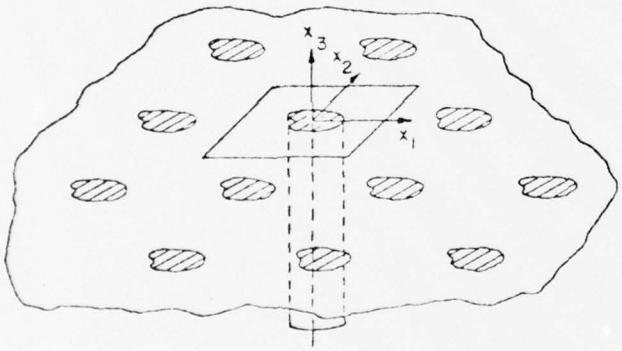

Fig. 3a

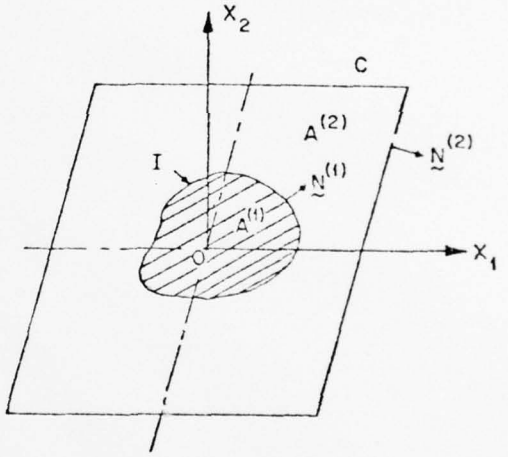

Fig. 3b

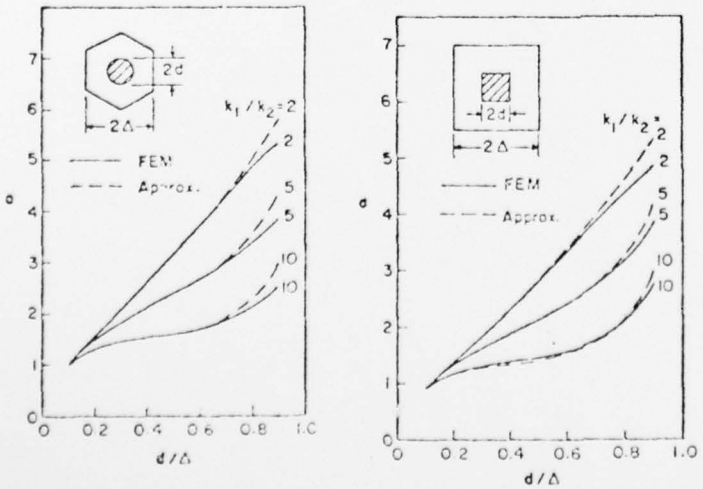

Fig. 4

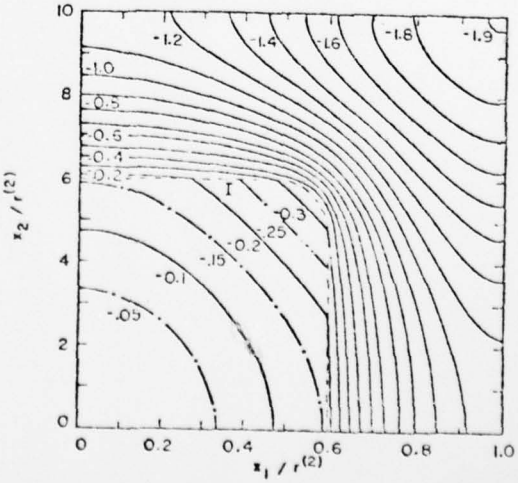

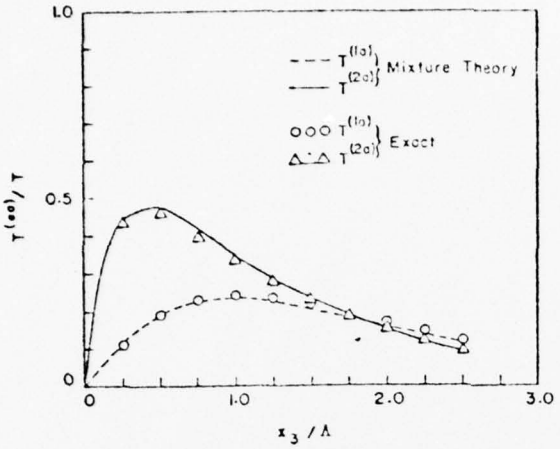

Fig. 5

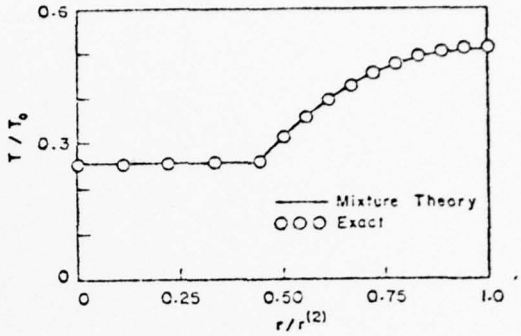

Fig. 6

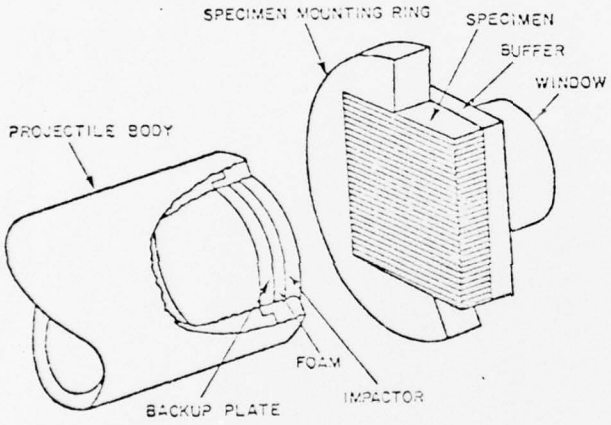

Fig. 7

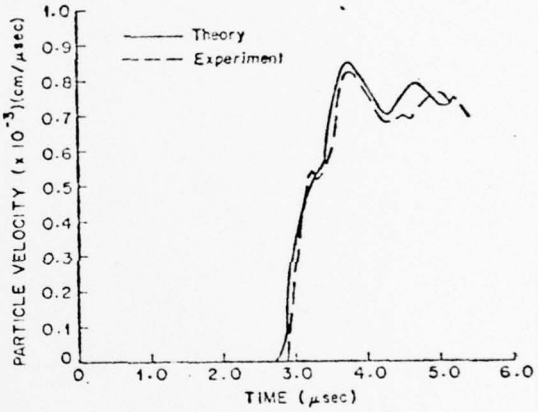

Fig. 8

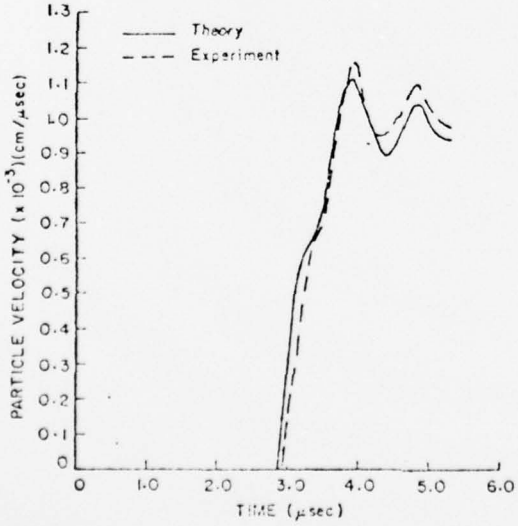

Fig. 9

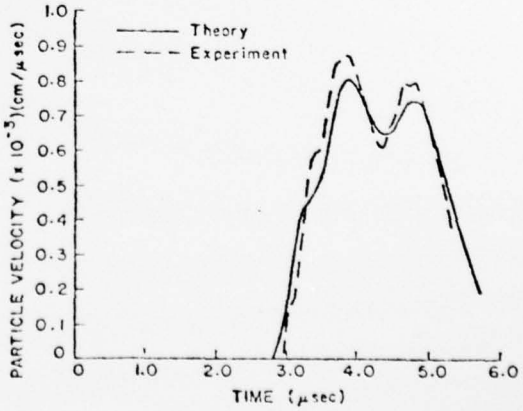

Fig. 10

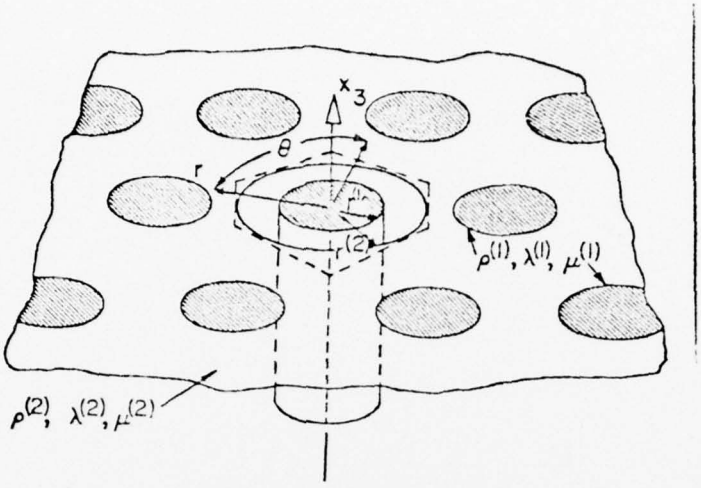

Fig. 11

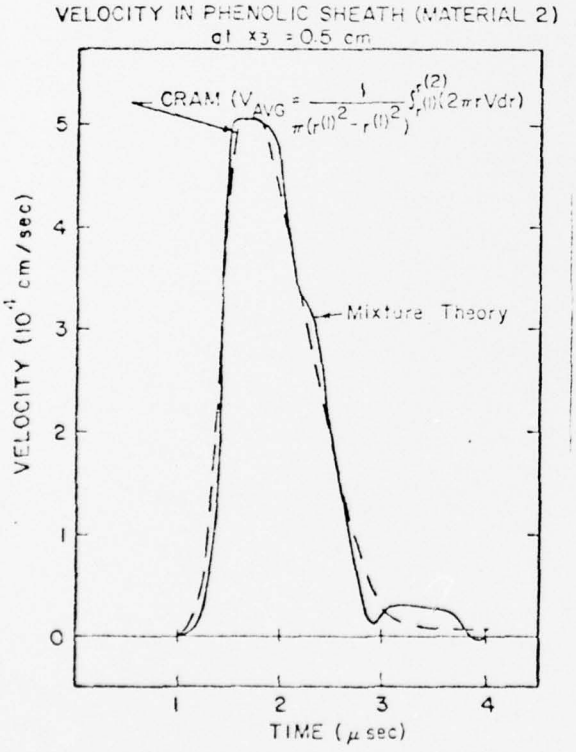

Fig. 12

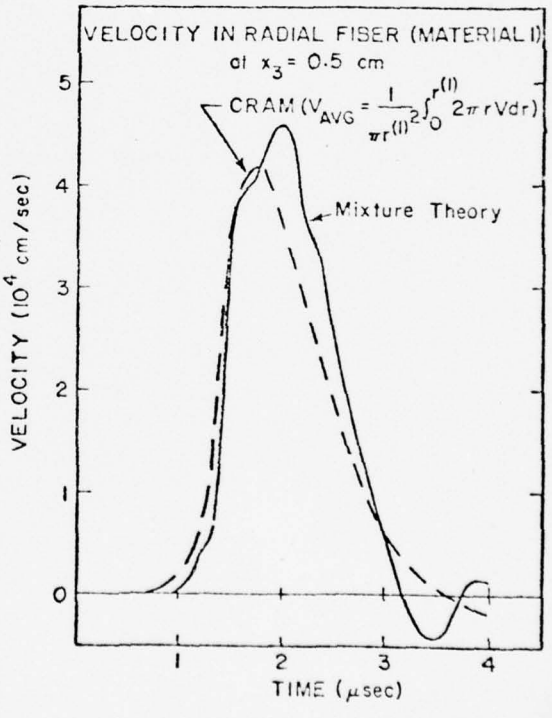

Fig. 13